Research Square

Preprints are preliminary reports that have not undergone peer review.
They should not be considered conclusive, used to inform clinical practice,
or referenced by the media as validated information.

Does the El Niño-Southern Oscillation Impact on the Indian Summer Monsoon 1-Dimensional? Quantifying the Role of Antecedent Southwestern Indian Ocean Capacitance on the Variability of Summer Monsoon Rainfall over Homogeneous Regions of India

Venugopal Thandlam (venux4@gmail.com)
Uppsala University
Hasibur Rahaman
Indian National Centre for Ocean Information Services
Anna Rutgersson
Uppsala University
Erik Sahlee
Uppsala University
Ravichandran Muthulagu
Ministry of Earth Sciences
Ramakrishna SSVS
Andhra University

Research Article

Keywords:

Posted Date: January 4th, 2022

DOI: https://doi.org/10.21203/rs.3.rs-1159437/v1

License: This work is licensed under a Creative Commons Attribution 4.0 International License.
Read Full License

Abstract

Recent rapid changes in the global climate and warming temperatures increase the demand for local and regional weather forecasting and analysis to improve the accuracy of seasonal forecasting of extreme events such as droughts and floods. On the other hand, the role of ocean variability is at a focal point in improving the forecasting at different time scales. Here we study the effect of Indian Ocean mean sea level anomaly (MSLA) and sea surface temperature anomalies (SSTA) on Indian summer monsoon rainfall during 1993-2019. While SSTA and MSLA have been increasing in the southwestern Indian Ocean (SWIO), these parameters' large-scale variability and pre-monsoon winds could impact the inter-annual Indian monsoon rainfall variability over homogeneous regions. Similarly, antecedent heat capacitance over SWIO on an inter-annual time scale has been the key to the extreme monsoon rainfall variability from an oceanic perspective. Though both SSTA and MSLA over SWIO have been influenced by El Niño-southern oscillation (ENSO), the impact of SWIO variability was low on rainfall variability over several homogeneous regions. However, rainfall over northeast (NE) and North India (NI) has been moulded by ENSO, thus changing the annual rainfall magnitude. Nevertheless, the impact of ENSO on monsoon rainfall through SWIO variability during the antecedent months is moderate. Thus, the ENSO influence on the atmosphere could be dominating the ocean part in modulating the inter-annual variability of the summer monsoon. Analysis shows that the cooler (warmer) anomaly over the western Indian Ocean affects rainfall variability adversely (favourably) due to the reversal of the wind pattern during the pre-monsoon period.

1. Introduction

The Indian summer monsoon variability on the inter-annual and intraseasonal time scale has puzzled the scientific community due to its complex, regionally heterogeneous variability (Gadgil et al., 2005; Rajeevan et al., 2012). With innovative technological advancement and many years of research, most dynamic and statistical models fail to predict the extremes and intra-seasonal monsoon rainfall variability with reasonable accuracy (Singh et al., 2019; Pradhan et al., 2017). This is due to the unpredictable variability within the monsoon system and the lack of understanding of the ocean’s role in Indian monsoon variability. It is also expected to the persistent ambiguity on the impact of the slowly responding ocean surface to the extreme atmosphere-ocean coupled phenomena such as El Niño-southern oscillation (ENSO) during the antecedent months and its imprint on the rainfall variability of the following year (Lau and Wang 2006; Heidelberg et al., 2005; Kug and Kang 2006). Thus, monsoon variability over homogeneous regions has not been examined despite the enhanced availability of observational data, especially satellite-derived sea surface temperature anomalies (SSTA), mean sea level anomalies (MSLA), and wind data over the global ocean extensively.

The Asian monsoon circulation influences most of the tropics and subtropics of the eastern hemisphere and more than 60% of the Earth’s population (Webster et al., 1998; Huang et al., 2016). Monsoon variations, mainly unanticipated, impart significant economic and social damages and consequences. Its failure often brings famine to affected regions, and strong monsoon years can result in devastating

floods (Christina et al., 2000). An accurate long-range seasonal and intra-seasonal predictions of monsoon rainfall can improve planning to mitigate monsoon variability's adverse impacts and benefit from beneficial conditions (Nisha et al., 2017; Webster et al., 1998). A better understanding of the monsoon cycle is clearly of scientific and social value.

Blanford (1884) was the first to attempt a forecast of the monsoon rainfall following the disastrous famine of 1877. The study was based on the hypotheses that the varying extent and thickness of the Himalayan snows exercise a tremendous and prolonged influence on the climatic conditions and weather of the plains of northwest India (Blanford, 1884). Much research has been done on forecasting all India summer monsoon rainfall (AISMR) (Kumar et al., 1995; Singh and Borah 2013; DelSole and Shukla 2012; Munot and Kumar 2007; Gadgil et al., 2002). Shukla (1975) suggested that colder SST anomalies over the western Arabian Sea and Somali coast may cause a reduction in monsoon rainfall over India and adjoining areas. Many studies also highlighted the positive correlations between sea surface temperature (SST) during pre-monsoon over the western Arabian Sea and monsoon rainfall for the better forecasting of AISMR (Cadet and Diehl 1984; Yu et al., 2021; Ratna et al., 2021; Valdivieso et al., 2021).

Several empirical studies show a strong positive correlation of Arabian Sea SST averaged over March, April, and May with AISMR (Shukla and Mooley 1987; Joseph and Pillai 1984; Rao and Goswami 1988; Allan et al. 1995). In addition, Harzallah and Sadourny (1997) investigated lag-lead relationships of global SST and the All-India Rainfall Index from 1950–90. In the fall and winter preceding a strong monsoon, they found positive SST anomalies in the Indian Ocean, especially the Arabian Sea.

On the time scale of the Tropical Biennial Oscillation, AISMR is significantly positively correlated with Indian Ocean SSTs and moisture flux transport in the preceding winter and spring seasons (Tim et al. 2001). Dash et al. (2002) examined the relationship of sea surface parameters such as SSTs, momentum flux and latent heat flux over the Arabian Sea, Bay of Bengal and the South China Sea with Indian monsoon rainfall. They reported that AISMR has a significant and positive correlation with the Arabian Sea's antecedent winter latent heat flux and SST anomalies. Vecchi and Harisson (2004) have shown that warm SSTA over the western Arabian Sea at the monsoon onset is associated with increased Western Ghat rainfall, while cool SSTA off Java and Sumatra is associated with increased precipitation over the Ganges-Mahanadi basin.

Kothawale et al. (2008) have found that November SST over the Arabian Sea, Bay of Bengal, and Equatorial South Indian Ocean is strongly correlated with AISMR during 1971-2002. Out of five homogeneous regions in India, monsoon rainfall over the West Coast of India (WCI) showed a significant relationship with Arabian Sea SSTs of the preceding spring and winter months. Also, Bay of Bengal SSTs preceding November and March and Equatorial South Indian Ocean SSTs of November, February, and March showed a substantial impact on WCI rainfall variability (Li et al., 2001; Izumo et al., 2008).

While most of the studies concentrated on relationships between SSTA over the Indian Ocean region and AISMR. Thus, very few studies have focussed on the relationship between Sea level variations and subsurface ocean variability over the Indian Ocean region and AISMR. Shankar and Shetye (1999) have

suggested that the interdecadal variability of sea level at Mumbai mimicked the variability in rainfall over the Indian subcontinent. The seasonal river outflow of the monsoon rainfall into the seas around India, and the dynamics of currents along the Indian coast, provides links between the rainfall over the Indian subcontinent and the sea level along the coast of India, with coastal salinity playing an intermediate role. Nevertheless, the reverse effect has not been studied for the monsoon rainfall variability. Similarly, ocean mean temperature, representing the heat energy of the upper ocean over the southwestern Indian Ocean (SWIO) during months of the same year, shows a strong statistical relationship with the AISMR (Ali et al., 2015). Furthermore, Venugopal et al. (2018) statistically illustrated that ocean mean temperature during January, February, and March over the SWIO could be a better ocean parameter for AISMR seasonal forecasting and variability during normal synoptic conditions. On the other hand, distinct impacts of short- and long-time fluctuations of the Indian Ocean surface wind fields, particularly over the SWIO, led to changes in the rainfall over homogeneous regions of India (Yangxing et al., 2020).

While monthly, seasonal, and regional rainfall contributes to the magnitude of AISMR, rainfall during July-August contributes to the total extent of seasonal rain, regardless of the strength (strong or weak) of the summer monsoon (Yangxing et al., 2016). Nevertheless, the strength of the monsoon and intraseasonal variability (MISO) depends on the prevailing synoptic conditions and intraseasonal variability of atmospheric and ocean parameters over the tropics, particularly in the tropical Indian and Pacific Oceans (Lie et al., 2007; Christopher and Webster 1999; Goswami et al., 2003). Recently Saha et al. (2019) have shown that the synoptic variability, considered noise, is predictable and has maximum contribution to the seasonal AISMR anomaly. Therefore, AISMR is a highly predictable system on a seasonal time scale. Furthermore, these synoptic activities and MISO, which are smaller in magnitude and affect the intensity of rainfall, are found to be associated with the planetary scale circulations like Madden-Julian Oscillation, ENSO, Indian Ocean Dipole, Pacific Decadal Oscillation and North Atlantic Oscillation (Krishnamurthy et al., 2014; Liebmann et al., 1994; Maloney and Hartmann, 2000; Saji et al. 1999; Webster et al., 1999; Sung et al., 2006). Thus, the predictability of AISMR lies on the planetary scale events, which evolve on a longer time scale and may leave their signature and impacts on the smaller-scale events to persist for a longer time (Saha et al., 2019).

While summer monsoon is a coupled atmosphere-ocean phenomenon, recent studies emphasised the role of air-sea interactions over southwestern and equatorial Indian Ocean as the key for the better understanding and forecasting of magnitude and variability of summer monsoon over India (Ali et al., 2015; Venugopal et al., 2018; Thandlam et al., 2020). Some of these studies stressed using new statistical techniques and parameters such as the strength of the winds, ocean heat content and ocean integrated subsurface temperatures in the seasonal forecasting of the summer monsoon (Yangxing et al., 2020; Venugopal et al., 2018). Though these studies found a relationship between summer monsoon and the upper ocean parameters over the SWIO concerning preceding months of the same year, none has focused on the relationship between rainfall over homogeneous regions of the Indian landmass and the SWIO. The question here is, does the Indian Ocean variability affect the entire Indian mainland ISMR? and how does the ENSO would affect this relationship? To the best of our knowledge, no studies are available about how the Indian Ocean variability impacts the different sub-divisions of India, popularly known as

homogeneous rainfall. The high ocean capacitance could hold the signature of planetary-scale events to persist for a more extended period, thus impacting the synoptic conditions in the following years. Hence, studying the role of antecedent upper ocean capacitance over the SWIO on AISMR and other homogeneous regions with and without the impact of planetary-scale events like ENSO could provide more insights into the influence of the air-sea interactions on synoptic conditions over this region. Furthermore, exploring the effect of the SWIO capacitance on homogeneous rainfall regions of India could give a more localised glance at physical processes and alter air-sea interactions due to recent climate change over these regions to changes in extreme floods and droughts (Sunitha et al., 2021, Thandlam et al., 2019). Also, quantifying the set of atmospheric and ocean parameters in seasonal numerical weather forecasting systems such as ECMWF's new long-range forecasting system SEAS5 is at high priority to improve the forecast precision.

On the other hand, a wide range of conflicting results has been described between Indian Ocean SST anomalies and Indian continental rainfall anomalies, which may partly arise because of uncertainties in our knowledge of Indian Ocean SST (Vecchi and Harrison, 2004). Much of the Indian Ocean is not well observed during various periods, either by satellite observations or ships and drifting buoys (Reynolds and Smith, 1994; Reynolds et al., 2002). Many studies have noted that statistical relations can be different in these modern decades than in earlier decades (Hastenrath, 1987; Torrence and Webster, 1999; Clark et al., 2000; Krishnamurthy and Goswami, 2000). The advent of satellite altimetry and microwave techniques to measure Sea Level Anomaly (SLA) and SST, respectively, have provided data sets with better spatial and temporal coverage over the Indian Ocean region in recent times.

In this study, we use these high spatial resolution datasets during 1993-2019 to determine the relationship between AISMR and SLA, SST before and after removing the Nino3.4 SST anomaly (SSTA) effect. A robust and distinct relationship with these parameters in the Indian Ocean has been found in recent years, especially after 2001 (Shi-Yun et al., 2021). We examined the role of these parameters over the SWIO in the rainfall variability of different homogeneous regions of India. Section 2 describes the datasets used and the methodology for the study. Subsequently, section 3 describes results and discussions. Finally, the conclusions are summarised in section 4.

2. Data And Methodology

2.1 Data

In recent times many studies have focused on the external forcing effect of Indian Ocean SST, especially from Arabian Sea SST to the Indian summer monsoon rainfall variability (Shukla 1975; Goswami and Rao, 1988; Vecchi et al. 2004; Kothawale et al. 2008). However, very few studies on the subsurface oceanic effect on the Indian summer monsoon rainfall. Under favourable conditions, the subsurface ocean thermal structure and heat content influence the air-sea interactions and the lower troposphere moisture content. Hence, the subsurface features in the SWIO, which are in the direct vicinity of the cross-equatorial winds before and during the summer monsoon, affect the rainfall over the land. Particularly,

ocean mean temperature during January-March over the SWIO up to 26^{o} isotherm derived from satellite altimeter data with great accuracy and has become an important parameter to study the variability of AISMR (Ali et al., 2015; Venugopal et al., 2018). However, despite satellite data, one of the discrepancies in using ocean data products such as ocean mean temperature and ocean heat content is the availability of reliable subsurface temperature and salinity data.

Meanwhile, sub-surface temperature and salinity profile data from scattered XBT, CTD, ARGO, and buoy's locations were previously available with spatial and temporal sampling errors. However, ARGO has recently made revolutions in this aspect by measuring T/S profile data since 2001 over the global ocean, including the Indian Ocean from 2003 (Gould et al., 2004; Ravichandran et al., 2004). Although the spatial distribution pattern of ARGO profiling floats was sparse during the initial phase, it has reached its objective to have at least one profile in a 3 x 3-degree domain in 2008 over the global ocean, including the Indian Ocean (Meyssignac et al., 2019). The other most reliable subsurface information comes from the sea level measurement since it shows the mirror image of subsurface variation in the surface. This data has been available from satellite altimetry with high spatial resolutions since 1992.

The high-resolution (0.25x0.25) blended analysis of daily Optimum Interpolation SST (OISSTv2.1, also known as Reynolds' SST) obtained from the National Oceanic and Atmospheric Administration (NOAA) during 1993-2019 (Reynolds et al., 2007) has been used in the study. In addition, we used delayed-time (reprocessed) daily SLA data for the 1993-2019 period with a spatial resolution of 0.25°, obtained from Copernicus Marine Environment Monitoring Service (CMEMS) (Rosmorduc et al., 2013). This product is obtained by combining fully processed data from various altimeter missions (Topex/Poseidon, ERS-1/2, Jason-1, Envisat and OSTM/Jason-2). The daily AISMR data has been extracted from the high-resolution (0.25 × 0.25) daily rainfall data constructed from more than 7000 rain gauge stations around India during the study period (Rajeevan et al., 2006; Pai et al., 2014). The AISMR data used in the study show a lower seasonal magnitude of rainfall than the data from Rajeevan et al., (2006) which has the 1^{o}x1^{o} resolution (figure not shown). The bias could be due to the annual changes in the number of rain gauge stations used in constructing the data. Despite its lower magnitude, the dataset has been used in the study owing to its higher spatial resolution. Based on the rainfall intensity and variability, homogeneous regions of AISMR are broadly divided into north India (NI), east India (EI), northeast India (NE), central India (CI), and WCI (Yangxing et al., 2016; Rahman and Sengupta 2007). Figure 1 shows the mean climatology of AISMR (June-September) during 1993-2019 in colour and the homogeneous rainfall regions. More details on the regions are provided in table 1. Similarly, the Nino3.4 (170W-120W and 5S-5N) region's monthly SSTA indices for ENSO were obtained from the Royal Netherlands Meteorological Institute climate explorer (Rayner et al., 2003). In addition, monthly surface zonal and meridional wind anomalies constructed from ECMWF-ERA5 with 0.25x0.25 resolution has been used in the composite analysis (Hersbach et al., 2017). Table 2 shows the details of the data used in the study.

Table 1: Details of homogeneous rainfall regions considered in the study.

Region name	Latitude-Longitude area	Short name	The seasonal mean of summer monsoon rainfall during 1993-2019 (mm)	The seasonal standard deviation of summer monsoon rainfall during 1993-2019 (mm)
All India Summer monsoon rainfall	Indian mainland	AISMR	529.3	362.5
West coast of India	71E-78E; 8N-22N with standard deviation > 3 mm/day	WCI	2178	338
North India	75.5E-80.5E; 28.5N-32.5N	NI	778.5	135.2
East India	84.5E-88.5E; 22.5N-28.5N	EI	1125	155.7
Northeast India	88.5E-97E; 22N-30N	NE	1468	207.0
Central India	74.5E-86.5E; 16.5N-26.5N	CI	886	98.4

Among the five homogeneous regions considered in the study, WCI and NE have the highest seasonal rainfall (figure 1) and standard deviation (Table 1), followed by EI, CI and NI. Hence, a seasonal departure from average rainfall over WCI and NE could influence the total AISMR magnitude. On the other hand, being a region with low standard deviation, the CI receives consistent seasonal rainfall and is also crucial for the absolute magnitude of the AISMR as CI covers a larger area than any other homogeneous region considered in the study.

Table 2: Details of data used in the study.

S.No	Parameter/Index	Grid spacing	Temporal resolution	Data Source	Study Region	Reference
1	All Indian Summer Monsoon Rainfall (AISMR)	0.25° × 0.25°	Daily	1	Indian mainland	Rajeevan et al., 2006; Pai et al., 2014
2	Sea surface temperature	0.25° × 0.25°	Daily	2	40°E–100°E, 30°S–30°N	Reynolds et al., 2007
3	Sea level anomaly	0.25° × 0.25°	Daily	3	40°E–100°E, 30°S–30°N	Rosmorduc et al., 2013
4	Nino3.4 (EL NIÑO) index	1° × 1°	Monthly	4	5°N–5°S, 170°W–120°W	Rayner et al., 2003
5	Zonal and meridional wind components	0.25° x 0.25°	Monthly	5	40°E–100°E, 30°S–30°N	Hersbach et al. (2017)

The availability of these data sets is different in time. However, for uniformity, the time period for all the datasets used was 1993-2019.

Date Source references: 1-India Meteorological Department; 2-National Oceanic and Atmospheric Administration; 3-Copernicus Marine Environment Monitoring Service; 4-Royal Netherlands Meteorological Institute; 5-Copernicus Climate Data Store (CDS).

2.2 Methodology

2.2.1 Identifying anomalous monsoon years

Krishnamurthy and Shukla (2000) have shown that the interannual variability of the Indian monsoon rainfall can be considered as a linear combination of a large-scale persistent seasonal mean component and a statistical average of intraseasonal variability in the gridded rainfall data. SST influences this large-scale persistent component. Therefore, the success in the long-range forecasting depends on accurate quantitative estimates of the externally forced component due to the intrinsically unpredictable intraseasonal component. Thus, our study looked at two external forcing fields SSTA and SSHA, over the Indian Ocean.

To identify the years of anomalous monsoon rainfall, we adopted Mooley and Parthasarathy's procedure (1983). The standard deviations for AISMR and the homogeneous regions of summer monsoon rainfall (June-September) were computed in the following way

$$\sigma_i = \frac{(R_i - R_m)}{\sigma_m} \qquad (1)$$

Where "σ_i" is the standard deviation of rainfall during the i^{th} year, "R_i" is the monsoon rainfall of the i^{th} year, "R_m" is the mean rainfall, and "σ_m" is the standard deviation of the monsoon rainfall during 1993-2019. These standard deviation values categorise monsoon rainfall as deficient or excess.

Deficient= $\sigma_i < -0.80$

Excess= $\sigma_i > 0.80$

The monthly anomaly fields for SLA and SST were constructed by computing monthly mean SLA and SST and then subtracting it from monthly climatology during 1993-2019. Table 3 shows the details of normal, deficit and excess monsoon years during the study period. Figure 2 shows the spatial pattern of summer monsoon rainfall standard deviation during 1993-2019. The regions with a standard deviation less than 4 mm/day in southern peninsular India, the northernmost part of India and northwestern India are considered rain shadow regions. These regions receive less rainfall during the summer monsoon. Thus, these regions' contribution to AISMR magnitude is minimal, not regarded as homogeneous regions.

Table 3: Details of the normal, deficit and excess summer monsoon rainfall years along with their standard deviation values during 1993-2019.

Excess years (σ_i)	Deficit years (σ_i)	Normal years (σ_i)	
1994 (1.453)	2000 (-0.881)	1993 (0.383)	2005 (-0.034)
2007 (1.217)	2002 (-2.202)	1995 (0.551)	2006 (0.675)
2011 (1.141)	2004 (-1.203)	1996 (0.082)	2008 (0.371)
2013 (1.217)	2009 (-1.871)	1997 (0.039)	2010 (0.748)
2019 (1.721)	2014 (-1.129)	1998 (0.506)	2012 (-0.197)
	2015 (-1.188)	1999 (-0.583)	2016 (0.201)
	2018 (-0.808)	2001 (-0.657)	2017 (0.023)
		2003 (0.685)	

Normal summer monsoon rains are present in 15 out of 27 years (55%) with standard deviation values between -0.8 and 0.8. On the other hand, 7 (26%) years received deficit monsoon, and 5 years received

excess summer monsoon rains (19%) in the study period. No deficit monsoon years were found in the first decade (1993-1999), but there was one year with the excess monsoon in 1994 and 6 normal monsoon years. The second decade (2000-2009) is more dynamic with 4 deficit years, one (2007) excess monsoon and 5 normal monsoon years. With the changing climate, the recent decade (2010-2019) witnessed the highest number of excess monsoon years in three decades (3) and the lowest number (4) of normal monsoon years, with 3 years being deficit monsoon years. Thus, in recent times monsoon rains show a significant deviation from normal rainfall magnitude and thus causing monsoon prediction to be more volatile and challenging.

2.2.2 Removal of ENSO effect on the relationship between Indian Ocean SSTA/MSLA and AISMR standard deviation

To remove the ENSO effect on the relationship between AISMR and SSTA/MSLA, we adopted the procedure of Kothawale et al. (2006). The influence of Nino3.4 is removed with the following equation

$$r_{123} = \frac{(r_{12} - r_{13} * r_{23})}{\sqrt{((1 - r_{13}^2) * (1 - r_{23}^2))}} \qquad (2)$$

where,

r_{123}: Correlation between SSTA/MSLA over the Indian Ocean and AISMR standard deviation excluding the effect of Nino3.4

r_{12}: Correlation between SSTA/MSLA over the Indian Ocean and AISMR standard deviation

r_{23}: Correlation between AISMR standard deviation and Nino3.4 SSTA indices

r_{13}: Simultaneous correlation between Indian Ocean SSTA/MSLA and Nino3.4 SSTA indices

The simultaneous monthly correlations between Indian Ocean SSTA and Indian Ocean MSLA with Nino3.4 SSTA indices are shown in figure 3a and figure 3b, respectively. Nino3.4 SSTA indices measure the occurrence and intensity of ENSO. While each ENSO event is unique, the intensity of a typical ENSO event would last for 9-12 months, with its lifecycle being about 4 years (Lin and Qian, 2019; Larkin and Harrison, 2002). A typical ENSO starts during boreal summer (Mar-Jun) and peaks during boreal winter (Dec-Feb) (Wang and Fiedler, 2006; Diaz et al., 2001). Hence, we computed the spatial correlation in the Indian Ocean concerning Nino3.4 SSTA from previous years June month. Starting from September, both SSTA and MSLA over SWIO show a positive correlation ($r>0.5$) with Nino3.4. These correlations spread through the south and north of the equatorial Indian Ocean in the later months and started to diminish after April, the following year. Hence, the Nino3.4 SSTs impact the SWIO and surrounding ocean regions during the preceding winters with strong intraseasonal to interannual variability. With the large heat capacitance of ocean waters, the SWIO may continue to affect the air-sea interactions over this region during later months and thus alter the rainfall in the following summer monsoon (Du et al., 2009; Schott

et al., 2009). Hence, improved monsoon forecasting would be possible with a deeper understanding of the role of SSTA and MSLA of SWIO on the homogeneous rainfall regions of India.

3. Results

3. 1 SSTA and MSLA variability and Monsoon rainfall

Figure 4 shows the changes (linear trend) in the summer monsoon rainfall, SST and SLA during 1993-2019. The WCI, NI, NE and EI together show a negative trend (-5 mm/day) in the monsoon rainfall during the study period (figure 4a). On the other hand, parts of WCI and NE show an increase of 5 mm/day rainfall during the study period. While the trend is neutral over other parts of India, the decreasing trend in the summer monsoon rainfall over NE, EI, and WCI might lead to a negative rainfall anomaly and drought-like condition over these regions. Changing synoptic conditions and remote forcing, together with local climate change, have increased the frequency of extreme rainfall, flash floods, glacier collapse and avalanches in the Himalayan regions in recent decades (Raj et al., 2021; Sigdel and Ma 2017; Singh and Goyal., 2016). These extremes in rainfall over these regions further cause landslides, damage to property and infrastructure and loss of lives. Thus, understanding precipitation variability more locally is gaining importance.

Similarly, while SLA over the SWIO showed a positive trend of 0.3-0.5 cm (figure 4c) in 27 years, SST showed a 1-1.2^{o}C increase (figure 4b) at the same time. The long-term rise in SLA over these regions implies that the thermocline became deeper, leading to an increase in SST. SWIO region also shows the most considerable intra-annual variability of upper ocean parameters among other parts of the global tropical oceans. Both SSTA and MSLA along the monsoonal low-level jet path in the SWIO show a substantial change from summer half-year (April-September) to winter half-year (October-March) (supplementary figures S1a, S1b). Thus, a slight change in the magnitude of these parameters over SWIO could lead to significant changes in air-sea interactions in the lower troposphere, cloud cover, variability in radiation and turbulent fluxes over this region. Though the difference in half-year wind speeds is moderate (supplementary figure S1c) over the region, the atmosphere saturated with water vapour and the influx of continuous moisture from the ocean into the atmosphere would lead to a healthy monsoon season.

During winter half-year, the southward movement of the intertropical convergence zone could lead to less insolation and ocean warming and change SSTA and MLSA over SWIO. Therefore, these changes in insolation and air-sea fluxes coupled with altering wind patterns would induce differences in SSTA and MSLA along the SWIO (figure S2). The increase in insolation due to northward propagation of intertropical convergence zone and increased wind speeds due to land-sea pressure gradient cause SSTA and MSLA to increase in summer months over SWIO (figure S2c and S2d). Nevertheless, SSTA standard deviation over SWIO is the highest in the Indian Ocean in winter half-year and summer months before summer monsoon full onset over India (figure 5a and 5b). During March-June, the large variability is associated with a robust cross-equatorial flow of winds over this region. This substantial variability on

the positive side over the region favours the evaporation and the magnitude of precipitation received over land in the following months (June-September). MSLA, on the other hand, shows moderate standard deviation values over the SWIO but has a significant standard deviation over the Seychelles-Chagos thermocline ridge region (Vialard et al., 2009) propagating from the southeast during winter half-year (figure 5c). The magnitude has become stronger during the summer months and reach the SWIO (figure 5d).

To identify the regions of large SSTA and MSLA variability which influences the monsoon rainfall, we choose the standard deviation of AISMR as an indication of large-scale monsoon activity. Xie et al. (2002) have shown that the thermocline variability over the SWIO affects the SST variability. This variability is due to the remotely controlled dynamical effects by phenomena like ENSO over the Pacific Ocean and IOD over the Indian Ocean (Saji et al. 1999). However, the effect may not be robust where the air-sea interaction process dominates the SST variability, especially over the SWIO, Arabian Sea and Bay of Bengal. Our results also corroborate this. Figure 6 shows the spatial correlation pattern between SSTA and SSHA. The correlation is high over the Seychelles-Changos thermocline ridge region. It is to be noted that simultaneous and lagged correlation patterns retain almost similar features; this suggests that the effect of SSHA on SSTA is due to the change of thermocline depth over this region.

3.1.1 Correlation between AISMR standard deviation and SSTA

We correlated the standard deviation of AISMR with the preceding year (-1) June month to current year (0) September month's SSTA and MSLA over the Indian Ocean. Figure 7 shows the spatial lagged correlation with values higher than +/- 0.2 significant at 95% level between AISMR standard deviation and SSTA. The correlation coefficients (CC) were computed between current years AISMR and SSTA from past June to present May. It shows that the current year's SST over the central Arabian Sea and the eastern equatorial Indian Ocean, which is connected to the Indo-Pacific warm pool, can affect the following year's monsoon. This may be because of persistent warm waters and ocean eddies life cycles over these regions. The lagged correlation shows maximum values over the SWIO during December-January, which started to evolve during preceding September. These correlations were diminished by March of the current year but appeared over the southwestern Arabian Sea during May, favouring the monsoon onset over the west coast of India. High correlations over the southwestern Arabian Sea corresponds to strong upwelling caused by the winds during this time (Izumo et al., 2008). So, observing and understanding prevailing synoptic conditions over this region until February could lead to better seasonal forecasting of the Indian summer monsoon (Rajendran et al., 2021). Also, this gives sufficient lead time for the seasonal prediction of Indian monsoon rainfall together with homogeneous regions.

To verify how the SSTA over the SWIO (40-65 E, 10S-10N) affects the AISMR, the time series of SSTA over SWIO has been analysed. Figure 8 shows the time series of SSTA over SWIO and AISMR standard deviation. The performance of AISMR is related to the SSTA anomaly over SWIO. Among other atmosphere-ocean factors, the increasing trend in SSTA in recent times could be one of the reasons favouring the large interannual variability of AISMR. These results differ slightly from the similar work of

Vecchi et al. (2004) and Izumu et al. (2008). However, this result corroborates the finding of Simon et al. (2008). The robustness of the relationship can be attributed to evaporative moisture flux from this region due to high wind stress (Venugopal et al., 2018). Earlier studies show that the bulk of the water vapour flux comes from the 10-20 S zonal belts, including the SWIO region above (Cadet et al., 1987; Kumar et al., 1986).

The role of Indian Ocean SST in affecting the total AISMR rainfall has been discussed in several previous studies (Rajeevan et al., 2002; Tripathi et al., 2008; Yu et al., 2021; Shahi et al., 2019). On the other hand, Venugopal et al. (2018) and Ali et al. (2015) showed that ocean mean temperature derived from ocean heat content over SWIO could be a better oceanic predictor for AISMR. Nevertheless, the question remains: Do the SWIO SST and subsurface dynamics (MSLA) affect the summer monsoon rainfall over the entire Indian landmass or only the homogeneous regions? To the best of our knowledge, no such studies have reported how the SWIO SST and MSLA will affect the different subregions of rainfall. Figure 9 shows the time series (red line) of lagged correlation between SSTA over SWIO and regional rainfall over the five homogeneous regions and entire Indian landmass. Out of five homogeneous regions in figure 9, the monsoon rainfall over the NI, CI and WCI was affected by SSTA changes over SWIO (Vecchi et al. 2004). On the other hand, these regions get most of their annual rainfall only during the southwest monsoon season. They showed rainfall over Gangetic plains, and the west coast of India is related to SST over the south Indian Ocean during Oct-Nov of the previous years.

A large part of the interannual variability of monsoon rainfall is linked to ENSO, a coupled ocean-atmospheric phenomenon in the Pacific Ocean. This phenomenon leads to the large-scale displacement of the east-west circulation in the tropics, influencing global SSTs (Walker, 1918; Pant and Rupa Kumar, 1997). Given this, the impact of ENSO on the relationship between Indian Ocean SSTA/MSLA and AISMR standard deviation has been examined by removing the influence of the ENSO effect. We consider the Nino3.4 region SSTA as the indicator of the ENSO phenomena. The ENSO effect has been removed following the methods described in sec 2.2.2. Figure 9 also shows the time series of these lagged correlations (blue line) computed between SSTA over SWIO and different homogeneous regions after removing the ENSO effect. The correlation values of AISMR and many other homogeneous regions show no significant difference from those observed without removing the ENSO effect. However, rainfall over the NE region is sensitive to the ENSO (Kumar et al., 2007; Saha et al., 2021), with significant differences in correlations. Hence it can be concluded that the SSTA anomaly over SWIO affects indigenously to the AISMR, especially over NI and CI.

Similarly, Figure 10a shows the monthly lagged cross-correlation between AISMR standard deviation and SSTA averaged over SWIO (40-65 E) along 30S-30N. It shows that the decorrelation length is ~3 months starting from March. These values are significant at 95% based on a student's t-test. Monthly lagged cross-correlation between AISMR standard deviation and SSTA averaged over 10S-10N shown in figure 10b shows that the decorrelation length is localised over SWIO with a time length of ~3 months in pre-monsoon. Both cases highlight the significant correlations over SWIO during the preceding autumn and winter months.

3.1.2 Correlation between AISMR standard deviation and MSLA

To know whether it is only due to the air-sea interaction process or subsurface temperature also does have any role, the SSHA from merged Altimeter data has been studied. SSHA variability gives the proxy of sub-surface temperature variability. Figure 11 shows the monthly lagged cross-correlations between AISMR and MSLA from June (-1) to September (0) over the Indian Ocean. This indicates that the mesoscale eddies have a dominant role in the monsoon variability. Their CC values are significant at a 90 % level based on the student's t-test analysis. Therefore, the increasing trend in the MSLA over SWIO, as shown in figure 12, potentially influences the positive trend in SSTA over the region due to strong surface winds, oceanic convective mixing, and air-sea flux exchanges. Mechanisms about how these eddies are influencing the Indian summer monsoon will be studied in detail in our future studies.

The correlation values over SWIO were increased during preceding October and continued until the current year's May. Thus, the sub-surface effects dominate during pre-monsoon time, as in the case of SSTA. The CC values above 90% significant levels are also observed over SWIO. This suggests that air-sea interactions over the surface, subsurface ocean dynamics and thermodynamics play a crucial role in the AISMR variability.

From the time series of AISMR standard deviation and SSHA over SWIO, AISMR standard deviation follows the SSHA variations (Figure 13). This relationship became robust during recent decades. This may be because Indian Ocean climate variability has become more active during the last couple of decades due to many positive Indian Ocean Dipoles (Saji et al. 1999; Rao et al. 2008). Like SSTA, the lagged correlation time series between AISMR standard deviation and MSLA over SWIO shows robust SSHA effects on the regional rainfall (Figure 13). AISMR and SSHA show maximum positive CC values in preceding December and during the current year's May. Except for NE and WCI, rainfall over all other homogeneous regions shows no large coupling with MSLA variability over SWIO. While CC of NE rainfall and MSLA strongly impact ENSO, the CC values over other regions remain unchanged after removing the ENSO effect (figure 13). However, the impact of MSLA variability over WCI and NE could influence the AISMR interannual variability due to the large share of the rainfall over the two regions in AISMR magnitude.

Figure 14a shows the lagged cross-correlations between AISMR standard deviation and SSHA averaged 40-65E. It shows two maxima, one around previous year's Oct-Nov and the other around Feb-Mar, lasting until Aug-Sep. The decorrelation scale is persistent over 15-20S. However, the average over 10S-10N (figure 14b), shows the decorrelation scale to propagate eastward from pre-monsoon months to the end of the same monsoon season (figure 14b). Thus, the SSHA variations over 40-65E and 10S-10N have a significant role in the AISMR variability. The observed high simultaneous correlation values between AISMR and MSLA during summer monsoon time supports the hypothesis of Shankar and Shetye (1999). Accordingly, the seasonal inflow of the monsoon rainfall into the seas around India and the dynamics of currents along the Indian coast provide the link between the rainfall over the Indian subcontinent and the sea level along the coast of India, with coastal salinity playing an intermediate role.

3.2 SSTA and MSLA variability during contrasting monsoon

To delineate the extreme monsoon rainfall variability, we have defined the excess, normal and drought years according to Mooley and Parthasarathy (1983). Figure 15 shows the composite of SSTA, MSLA (shaded) and sea surface wind (vector) for excess, deficit, and normal monsoon years. During excess monsoon years, both SSTA and MSLA are positive over the SWIO, including the Seychelles-Chagos thermocline ridge region. Anomalous weak surface winds (near the east African coast) with the north-easterly flow instead of normal south-westerlies favours these conditions over the region. This anomalous weak wind reduces the upwelling, and the region becomes one of the moisture source regions during the subsequent monsoon months (Izumo et al. 2008). The MSLA variability can be taken as a proxy to ocean heat content. The positive MSLA over the entire SWIO with shallow mixed and deep isothermal layers could act as a heat source for the moisture supply.

In contrast, the composite during the deficit monsoon year's shows an opposite spatial pattern of SSTA, MSLA and reversal of winds over the entire Indian Ocean. Both SSTA and MSLA over SWIO, including the Seychelles-Chagos thermocline ridge region, turned unfavourable with strong westerly winds. The negative MSLA signifies the deep MLD and shallow thermocline over these regions. Normal monsoon years are accompanied by the moderate values of SSTA, MSLA and winds, which could lead to dampened air-sea flux exchange between the upper ocean and the lower troposphere over the Indian Ocean. The wind anomalies from National Centers for Environmental Prediction (NCEP) daily reanalysis 2 data with 2.5x2.5 resolution (Kalnay et al., 1996) also show similar results (not shown here).

4. Conclusions And Discussions

The availability of high spatial resolution satellite altimetry and microwave SST data opened windows to undertake a detailed study of Indian Ocean dynamics and understand the synoptic conditions over the region. Thereby there is an increasing interest in several phenomena in the Indian Ocean that impacts global weather and climate at different temporal and spatial scales. Among others, IOD, MJO and tropical cyclones are a few coupled events influenced by Indian Ocean synoptic conditions. Similarly, All India summer monsoon rainfall (AISMR) is another major annual event that strongly impacts the atmosphere and oceanic conditions. While the atmosphere controls a large part of the monsoon dynamics, the ocean's role in interannual summer rainfall variability is unavoidable. Several recent studies emphasised the impact of pre-monsoon SST and upwelling over the Arabian Sea and the tropical Indian Ocean (Athira and Abhilash 2021; Jayaram et al., 2010; Gnanaseelan et al., 2005). In addition, a few recent studies explored the role of subsurface variability in the form of ocean heat content; ocean mean temperature and sea-level changes on AISMR (Venugopal et al., 2018; Ali et al., 2015).

On the other hand, contemporary trends in climate change, changes in surface and air temperatures are causing the large interannual variability in AISMR magnitudes, thus causing more frequent droughts and floods. These changes in both atmosphere and oceanic variables also increase the intensities of planetary-scale events such as ENSO. With large heat capacitance, oceans could impact these global-

scale phenomena longer and affect the air-sea fluxes in the subsequent months. The SWIO is one such region, influenced by events like MJO, IOD and ENSO.

Though several studies attempted to understand the impact of these processes on the variability of AISMR magnitude, the majority of previous works have either focused on the total variability of AISMR or considered single or multiple ocean parameters to study the contemporary relationship with AISMR. Thus, limited attempts were made to understand the connection between rainfall variability over homogeneous regions and oceanic parameters in the Indian Ocean influenced by the events like ENSO during the preceding months. Hence finding the relationship between preceding months (previous year June to following year May) Indian Ocean heat capacitance and monsoon rainfall over different homogeneous regions in the following year could improve the monsoon forecasting in the near future. In addition, we also studied the impact of ENSO on the connections among SSTA, MSLA and rainfall over land.

Wind-induced mixing and upwelling over SWIO during May and April (prior to monsoon onset) led to a robust lead-lag correlation between MSLA and SSTA over the region. Thus, the strong coupling between MSLA and SSTA over SWIO led to strong seasonal variability of these two parameters over the region. Reversal of winds, changes in upper ocean parameters and altering insolation twice a year due to movement of thermal equator made the SWIO region unique among other parts of the global tropical ocean with the highest SST and SLA variability from winter to summer half-year. Thus, these two parameters show a sizeable standard deviation over SWIO. Also, the occurrence of IOD and ENSO affects the air-sea interactions over SWIO and induce changes in the SST and SLA. The simultaneous correlations of Nino3.4 SSTA with both SSTA and MSLA over the Indian Ocean show large values over the region. Furthermore, the ocean heat advecting from the Southern Ocean warming (Gille 2002) could be causing warming and the positive trends in SSTA and MSLA over SWIO.

SWIO heat capacitance in the form of variability in SSTA and MSLA during preceding autumn and winter months could induce sizeable inter-annual variability of summer monsoon over Indian landmass. Surface temperatures over SWIO from the prior year's September (-1) to the current years' February (0) month show better correlations with AISMR standard deviation. The correlations have become more prominent over the Arabian Sea during May (0) but leave no time for the monsoon's seasonal prediction. Though ENSO impact was moderate, rainfall over NI and CI were strongly associated with SSTA variability. The NE rainfall has a significant effect due to the ENSO effect over SWIO. While SSTA and rainfall standard deviation correlations have a decorrelation length of 3 months, rainfall correlations with MSLA show bi-modal oscillation with peaks in autumn and fall. The MSLA and rainfall correlations over SWIO were low during January (0). However, the increased correlations from February (0) have eastward propagation until the end of monsoon season in September (0). The NE and WCI regions show large rainfall variability due to MSLA over SWIO.

On the other hand, excess monsoon can be expected with positive MSLA, SSTA and associated low and reverse wind anomalies over the East African coast. Opposite MSLA, SSTA conditions with strong westerlies over SWIO could lead to deficit summer monsoon rainfall. Normal monsoon years are

associated with neutral magnitudes of these parameters over SWIO. Finally, the impact of ENSO on the variability of homogeneous rainfall through induced changes in SSTA and MSLA over SWIO was moderate. The weakened feedback of the Indian Ocean on ENSO since the early 1990s could also be a key here (Han and Wang 2021). These findings signify that SWIO antecedent heat capacitance in SSTA and MSLA is moderate over homogeneous rainfall regions, with some regions showing negative correlations. However, the impact of ENSO on atmospheric conditions over the Indian Ocean could be more significant than that on ocean parameters over SWIO in modulating inter-annual variability of AISMR.

5. Data Availability

All data used in the study are freely available. Rainfall data can be obtained from India Meteorological Department (https://www.imdpune.gov.in/Clim_Pred_LRF_New/Grided_Data_Download.html). Sea surface temperature data was downloaded from National Oceanic and Atmospheric Administration (https://www.ncei.noaa.gov/products/optimum-interpolation-sst). Sea level anomaly data are obtained from Copernicus Marine Environment Monitoring Service (https://marine.copernicus.eu). Royal Netherlands Meteorological Institute hosts the NINO3.4 indices (https://climexp.knmi.nl/selectindex.cgi). ERA5 surface wind data was downloaded from the C3S climate data store (CDS) (https://cds.climate.copernicus.eu/cdsapp#!/dataset/reanalysis-era5-single-levels?tab=overview) and NCEP reanalysis from National Centers for Environmental Prediction (https://psl.noaa.gov/data/gridded/data.ncep.reanalysis.pressure.html).

6. Code Availability

The analysis was done using PyFerret developed by Pacific Marine Environment Laboratory, National Oceanic and Atmospheric Administration (https://ferret.pmel.noaa.gov/Ferret). The analysis codes used in this study are available from the corresponding author upon request.

7. References

1. Ali, M. M., Nagamani, P. V., Sharma, N., Venu Gopal, R. T., Rajeevan, M., Goni, G. J., & Bourassa, M. A. (2015). Relationship between ocean mean temperatures and Indian summer monsoon rainfall. Atmospheric Science Letters, 16(3), 408-413.
2. Athira, U. N., & Abhilash, S. (2021). Ocean–atmosphere coupled processes in the tropical Indian Ocean region prior to Indian summer monsoon onset over Kerala. Climate Dynamics, 56(1), 597-612.
3. Clark, Christina Oelfke, Julia E. Cole, and Peter J. Webster. "Indian Ocean SST and Indian summer rainfall: Predictive relationships and their decadal variability." Journal of Climate 13, no. 14 (2000): 2503-2519.
4. DelSole, T., & Shukla, J. (2012). Climate models produce skilful predictions of Indian summer monsoon rainfall. Geophysical Research Letters, 39(9).

5. Diaz, H. F., Hoerling, M. P., & Eischeid, J. K. (2001). ENSO variability, teleconnections and climate change. International Journal of Climatology: A Journal of the Royal Meteorological Society, 21(15), 1845-1862.
6. Du, Y., Xie, S. P., Huang, G., & Hu, K. (2009). Role of air–sea interaction in the long persistence of El Niño–induced north Indian Ocean warming. Journal of Climate, 22(8), 2023-2038.
7. Friedrich A. Schott, Shang-Ping Xie and Julian P. McCreary Jr, “Indian Ocean Circulation and Climate Variability,” Rain, vol. 47, no. 2007, pp. 1–46, 2009.
8. G. Alory, S. Wijffels, and G. Meyers, “Observed temperature trends in the Indian Ocean over 1960–1999 and associated mechanisms,” Geophys. Res. Lett., vol. 34, no. 2, p. L02606, Jan. 2007.
9. G. Turner and H. Annamalai, “Climate change and the South Asian summer monsoon,” Nat. Clim. Chang., vol. 2, no. 8, pp. 587–595, Jun. 2012
10. Gadgil, S., Rajeevan, M., & Nanjundiah, R. (2005). Monsoon prediction–Why yet another failure?. Current science, 88(9), 1389-1400.
11. Gadgil, S., Srinivasan, J., Nanjundiah, R. S., Kumar, K. K., Munot, A. A., & Kumar, K. R. (2002). On forecasting the Indian summer monsoon: the intriguing season of 2002. Current Science, 83(4), 394-403.
12. Gille, S. T. (2002). Warming of the Southern Ocean since the 1950s. Science, 295(5558), 1275-1277.
13. Gnanaseelan, C., Thompson, B., Chowdary, J. S., & Salvekar, P. S. (2005). Evolution and collapse of Arabian Sea warm pool during two contrasting monsoons 2002 and 2003. Mausam, 56(1), 187-200.
14. Gould, J., Roemmich, D., Wijffels, S., Freeland, H., Ignaszewsky, M., Jianping, X., ... & Riser, S. (2004). Argo profiling floats bring new era of in situ ocean observations. Eos, Transactions American Geophysical Union, 85(19), 185-191.
15. Han, X., Wang, C. Weakened feedback of the Indian Ocean on ENSO since the early 1990s. Clim Dyn 57, 879–894 (2021). https://doi.org/10.1007/s00382-021-05745-5
16. Yu, J. Y., & Lau, K. M. (2005). Contrasting Indian Ocean SST variability with and without ENSO influence: A coupled atmosphere-ocean GCM study. Meteorology and Atmospheric Physics, 90(3), 179-191.
17. Hersbach, H., Bell, B., Berrisford, P., Hirahara, S., Horányi, A., Muñoz-Sabater, J., ... & Schepers, D. (2017). Complete ERA5: Fifth Generation of ECMWF Atmospheric Reanalyses of the Global Climate. Copernicus Climate Change Service (C3S) Data Store (CDS).
18. Huang, Jianping, Mingxia Ji, Yongkun Xie, Shanshan Wang, Yongli He, and Jinjiang Ran. "Global semi-arid climate change over last 60 years." Climate Dynamics 46, no. 3-4 (2016): 1131-1150.
19. Izumo, T., Montégut, C. B., Luo, J. J., Behera, S. K., Masson, S., & Yamagata, T. (2008). The role of the western Arabian Sea upwelling in Indian monsoon rainfall variability. Journal of Climate, 21(21), 5603-5623.
20. Izumo, T., Montégut, C. B., Luo, J. J., Behera, S. K., Masson, S., & Yamagata, T. (2008). The role of the western Arabian Sea upwelling in Indian monsoon rainfall variability. Journal of Climate, 21(21),

5603-5623.

21. J. G. Charney and J. Shukla, Monsoon dynamics. Cambridge: Cambridge University Press, 1981.
22. J. Namias and D. R. Cayan, “Large-Scale Air-Sea Interactions and Short-Period Climatic Fluctuations,” Science (80.)., vol. 214, no. 4523, pp. 869–876, Nov. 1981
23. Jayaram, C., Chacko, N., Joseph, K. A., & Balchand, A. N. (2010). Interannual variability of upwelling indices in the southeastern Arabian Sea: a satellite based study. Ocean Science Journal, 45(1), 27-40.
24. K. N. Kumar, M. Rajeevan, J. Srinivasan, C. Gnanaseelan, and M. M. Ali, “Objective Database Epochal variations of Arabian Sea TCs Vertical Wind Shear WORKSHOP ON INTERDECADAL VARIABILITY OF THE GLOBAL MONSOONS , 10 – 12 September 2012 , Nanjing , China,” p. 5601012, 2012.
25. Kalnay, Eugenia, Masao Kanamitsu, Robert Kistler, William Collins, Dennis Deaven, Lev Gandin, Mark Iredell et al. "The NCEP/NCAR 40-year reanalysis project." Bulletin of the American meteorological Society 77, no. 3 (1996): 437-472.
26. Krishnamurthy, Lakshmi, and V. J. C. D. Krishnamurthy. "Influence of PDO on South Asian summer monsoon and monsoon–ENSO relation." Climate Dynamics 42, no. 9-10 (2014): 2397-2410.
27. Kug, J. S., & Kang, I. S. (2006). Interactive feedback between ENSO and the Indian Ocean. Journal of climate, 19(9), 1784-1801.
28. Kumar, K. K., Soman, M. K., & Kumar, K. R. (1995). Seasonal forecasting of Indian summer monsoon rainfall: a review. Weather, 50(12), 449-467.
29. Kumar, M. R., Sathyendranath, S., Viswambharan, N. K., & Rao, L. G. (1986). Sea surface temperature variability over North Indian Ocean—A study of two contrasting monsoon seasons. Proceedings of the Indian Academy of Sciences-Earth and Planetary Sciences, 95(3), 435-446.
30. Kumar, P., Kumar, K. R., Rajeevan, M., & Sahai, A. K. (2007). On the recent strengthening of the relationship between ENSO and northeast monsoon rainfall over South Asia. Climate Dynamics, 28(6), 649-660.
31. Kurian, Nisha, T. Venugopal, Jatin Singh, and M. M. Ali. "A soft-computing ensemble approach (SEA) to forecast Indian summer monsoon rainfall." Meteorological Applications 24, no. 2 (2017): 308-314.
32. Larkin, N. K., & Harrison, D. E. (2002). ENSO warm (El Niño) and cold (La Niña) event life cycles: Ocean surface anomaly patterns, their symmetries, asymmetries, and implications. Journal of climate, 15(10), 1118-1140.
33. Lau, N. C., & Wang, B. (2006). Interactions between the Asian monsoon and the El Nino/Southern oscillation. In The Asian Monsoon (pp. 479-512). Springer, Berlin.
34. Li, T., Zhang, Y., Chang, C. P., & Wang, B. (2001). On the relationship between Indian Ocean sea surface temperature and Asian summer monsoon. Geophysical Research Letters, 28(14), 2843-2846.
35. Li, Ying, Riyu Lu, and Buwen Dong. "The ENSO–Asian monsoon interaction in a coupled ocean-atmosphere GCM." Journal of Climate 20, no. 20 (2007): 5164-5177.
36. Lin, I. I., Goni, G. J., Knaff, J. A., Forbes, C., & Ali, M. M. (2013). Ocean heat content for tropical cyclone intensity forecasting and its impact on storm surge. Natural hazards, 66(3), 1481-1500.

37. Lin, J., & Qian, T. (2019). A new picture of the global impacts of El Nino-Southern oscillation. Scientific reports, 9(1), 1-7.
38. M. J. McPhaden, “The Global Tropical Moored Buoy Array,” Proc. Ocean. Sustain. Ocean Obs. Inf. Soc., no. 1, pp. 668–682, 2010.
39. M. M. Ali, D. Swain, T. Kashyap, J. P. McCreary, and P. V. Nagamani, “Relationship Between Cyclone Intensities and Sea Surface Temperature in the Tropical Indian Ocean,” IEEE Geosci. Remote Sens. Lett., vol. 10, no. 4, pp. 841–844, Jul. 2013.
40. M. M. Ali, T. Kashyap, and P. V. Nagamani, “Use of Sea Surface Temperature for Cyclone Intensity Prediction Needs a Relook,” Eos, Trans. Am. Geophys. Union, vol. 94, no. 19, pp. 177–177, May 2013.
41. M. Rajeevan, D. S. Pai, R. Anil Kumar, and B. Lal, “New statistical models for long-range forecasting of southwest monsoon rainfall over India,” Clim. Dyn., vol. 28, no. 7–8, pp. 813–828, Nov. 2006.
42. M. Roxy, “Sensitivity of precipitation to sea surface temperature over the tropical summer monsoon region and its quantification,” Clim. Dyn., vol. 43, no. 5–6, pp. 1159–1169, Jul. 2014.
43. Meyssignac, B., Boyer, T., Zhao, Z., Hakuba, M. Z., Landerer, F. W., Stammer, D., ... & Zilberman, N. (2019). Measuring global ocean heat content to estimate the Earth energy imbalance. Frontiers in Marine Science, 6, 432.
44. Mohanty, U. C., Sinha, P., Mohanty, M. R., Maurya, R. K. S., & RAO, M. N. (2019). A review on the monthly and seasonal forecast of the Indian summer monsoon. Mausam, 70(3), 425-442.
45. Munot, A. A., & Kumar, K. K. (2007). Long range prediction of Indian summer monsoon rainfall. Journal of earth system science, 116(1), 73-79.
46. N. H. Saji, B. N. Goswami, P. N. Vinayachandran, and T. Yamagata, “A dipole mode in the tropical Indian Ocean.,” Nature, vol. 401, no. 6751, pp. 360–363, 1999.
47. P. J. Webster, M. Moore, J. P. Loschnigg, and R. R. Leben, “Coupled ocean-atmosphere dynamics in the Indian Ocean during 1997-98.,” Nature, vol. 401, no. 6751, pp. 356–360, 1999.
48. P. Swapna, R. Krishnan, and J. M. Wallace, “Indian Ocean and monsoon coupled interactions in a warming environment,” Clim. Dyn., vol. 42, no. 9–10, pp. 2439–2454, May 2014.
49. Pai, D. S. et al. Development of a new high spatial resolution (0.25 × 0.25) long period (1901–2010) daily gridded rainfall data set over India and its comparison with existing data sets over the region. Mausam 65(1), 1–18 (2014).
50. Pradhan, M., Rao, A. S., Srivastava, A., Dakate, A., Salunke, K., & Shameera, K. S. (2017). Prediction of Indian summer-monsoon onset variability: A season in advance. Scientific reports, 7(1), 1-14.
51. R. T. Sutton, B. Dong, and J. M. Gregory, “Land/sea warming ratIndian Oceanin response to climate change: IPCC AR4 model results and comparison with observations,” Geophys. Res. Lett., vol. 34, no. 2, p. L02701, Jan. 2007.
52. Rahman, Hasibur, and Debasis Sengupta. "Preliminary comparison of daily rainfall from satellites and Indian gauge data." CAOS technical report 2007AS1 (2007).

53. Raj, S., Shukla, R., Trigo, R. M., Merz, B., Rathinasamy, M., Ramos, A. M., & Agarwal, A. (2021). Ranking and characterization of precipitation extremes for the past 113 years for Indian western Himalayas. International Journal of Climatology.
54. Rajeevan, M., Bhate, J., Kale, J. D. & Lal, B. High resolution daily gridded rainfall data for the Indian region: Analysis of break and active monsoon spells. Current Science, 296–306 (2006).
55. Rajeevan, M., Pai, D. S., & Thapliyal, V. (2002). Predictive relationships between Indian Ocean sea surface temperatures and Indian summer monsoon rainfall. Mausam, 53(3), 337-348.
56. Rajeevan, M., Unnikrishnan, C. K., & Preethi, B. (2012). Evaluation of the ENSEMBLES multi-model seasonal forecasts of Indian summer monsoon variability. Climate Dynamics, 38(11), 2257-2274.
57. Rajendran, K., Surendran, S., Varghese, S. J., & Chakraborty, A. (2021). Do seasonal forecasts of Indian summer monsoon rainfall show better skill with February initial conditions?. Current Science (00113891), 120(12).
58. Ratna, S. B., Cherchi, A., Osborn, T. J., Joshi, M., & Uppara, U. (2021). The extreme positive Indian Ocean Dipole of 2019 and associated Indian summer monsoon rainfall response. Geophysical Research Letters, 48(2), e2020GL091497.
59. Ravichandran, M., Vinayachandran, P. N., Joseph, S., & Radhakrishnan, K. (2004). Results from the first Argo float deployed by India. Current Science, 86(5), 651-659.
60. Rayner, N. A. et al. Global analyses of sea surface temperature, sea ice, and night marine air temperature since the late nineteenth century. Journal of Geophysical Research: Atmospheres, 108(D14) (2003).
61. Reynolds, R.W. et al (2007): Daily high-resolution blended analyses for sea surface temperature. J. Climate, 20 , 5473-5496.
62. Rosmorduc, V., Bronner, E., Maheu, C. & Mertz, F. Aviso: altimetry products and services in 2013. In EGU General Assembly Conference Abstracts, vol. 15 (2013).
63. S. A. Rao, A. R. Dhakate, S. K. Saha, S. Mahapatra, H. S. Chaudhari, S. Pokhrel, and S. K. Sahu, “Why is the Indian Ocean warming consistently?,” Clim. Change, vol. 110, no. 3–4, pp. 709–719, Jun. 2012.
64. S. Gadgil, M. Rajeevan, and R. Nanjundiah, “Monsoon prediction–Why yet another failure,” Curr. Sci., vol. 88, no. April 2016, pp. 1389–1400, 2005.
65. Saha, K., Guha, A., & Banik, T. (2021). Indian summer monsoon variability over North-East India: Impact of ENSO and IOD. Journal of Atmospheric and Solar-Terrestrial Physics, 221, 105705.
66. Saha, Subodh Kumar, Anupam Hazra, Samir Pokhrel, Hemantkumar S. Chaudhari, K. Sujith, Archana Rai, Hasibur Rahaman, and B. N. Goswami. "Unraveling the mystery of Indian summer monsoon prediction: Improved estimate of predictability limit." Journal of Geophysical Research: Atmospheres 124, no. 4 (2019): 1962-1974.
67. Saji, N. H., Bhupendra Nath Goswami, P. N. Vinayachandran, and T. Yamagata. "A dipole mode in the tropical Indian Ocean." Nature 401, no. 6751 (1999): 360-363.

68. Schott, F. A., Xie, S. P., & McCreary Jr, J. P. (2009). Indian Ocean circulation and climate variability. Reviews of Geophysics, 47(1).
69. Shahi, N. K., Rai, S., & Mishra, N. (2019). Recent predictors of Indian summer monsoon based on Indian and Pacific Ocean SST. Meteorology and Atmospheric Physics, 131(3), 525-539.
70. Sigdel, M., & Ma, Y. (2017). Variability and trends in daily precipitation extremes on the northern and southern slopes of the central Himalaya. Theoretical and Applied Climatology, 130(1), 571-581.
71. Singh, B., Cash, B., & Kinter III, J. L. (2019). Indian summer monsoon variability forecasts in the North American multimodel ensemble. Climate dynamics, 53(12), 7321-7334.
72. Singh, P., & Borah, B. (2013). Indian summer monsoon rainfall prediction using artificial neural network. Stochastic environmental research and risk assessment, 27(7), 1585-1599.
73. Singh, V., & Goyal, M. K. (2016). Changes in climate extremes by the use of CMIP5 coupled climate models over eastern Himalayas. Environmental Earth Sciences, 75(9), 839.
74. Sung, Mi-Kyung, Won-Tae Kwon, Hee-Jeong Baek, Kyung-On Boo, Gyu-Ho Lim, and Jong-Seong Kug. "A possible impact of the North Atlantic Oscillation on the east Asian summer monsoon precipitation." Geophysical Research Letters 33, no. 21 (2006).
75. Sunita Narain, Shazneen Cyrus Gazdar, Avantika Goswami and Tarun Gopalakrishnan, 2021, Climate Change: Science and Politics, Centre for Science and Environment, New Delhi
76. Thandlam, V., Rutgersson, A., & Rahaman, H. (2019). Are we in the right path in using early warning systems?. Journal of Extreme Events, 6(02), 1950003.
77. Thandlam, V., T.V.S, U.B., Hasibur, R. et al. A sea-level monopole in the equatorial Indian Ocean. npj Clim Atmos Sci 3, 25 (2020). https://doi.org/10.1038/s41612-020-0127-z.
78. Torrence, Christopher, and Peter J. Webster. "Interdecadal changes in the ENSO–monsoon system." Journal of climate 12, no. 8 (1999): 2679-2690.
79. Tripathi, K. C., Rai, S., Pandey, A. C., & Das, I. M. L. (2008). Southern Indian Ocean SST indices as early predictors of Indian summer monsoon.
80. V. Krishnamurthy and B. P. Kirtman, “Relation between Indian Monsoon Variability and SST,” J. Clim., vol. 22, no. 17, pp. 4437–4458, Sep. 2009.
81. Valdivieso, M., Peatman, S. C., & Klingaman, N. P. (2021). The influence of air–sea coupling on forecasts of the 2016 Indian summer monsoon and its intraseasonal variability. Quarterly Journal of the Royal Meteorological Society, 147(734), 202-228.
82. Venugopal, T., Ali, M. M., Bourassa, M. A., Zheng, Y., Goni, G. J., Foltz, G. R., & Rajeevan, M. (2018). Statistical evidence for the role of SWIO heat content in the Indian summer monsoon rainfall. Scientific reports, 8(1), 1-10.
83. Wang, C., & Fiedler, P. C. (2006). ENSO variability and the eastern tropical Pacific: A review. Progress in Oceanography, 69(2-4), 239-266.
84. Webster, P. J.,V. O. Magana, T. N. Palmer, J. Shukla, R. A. Tomas, M. Yanai,and T. Yasunari, 1998; Monsoons: Processes, predictability, and the prospects for prediction; J. Geophys. Res., 103, 14 451–

14 510.

85. Yu, S. Y., Fan, L., Zhang, Y., Zheng, X. T., & Li, Z. (2021). Reexamining the Indian Summer Monsoon Rainfall–ENSO relationship from its recovery in the 21st century: role of the Indian Ocean SST anomaly associated with types of ENSO evolution. Geophysical Research Letters, 48(12), e2021GL092873.
86. Yu, S. Y., Fan, L., Zhang, Y., Zheng, X. T., & Li, Z. (2021). Reexamining the Indian Summer Monsoon Rainfall–ENSO relationship from its recovery in the 21st century: Role of the Indian Ocean SST anomaly associated with types of ENSO evolution. Geophysical Research Letters, 48(12), e2021GL092873.
87. Yu, Shi-Yun, Lei Fan, Yu Zhang, Xiao-Tong Zheng, and Ziguang Li. "Reexamining the Indian Summer Monsoon Rainfall–ENSO relationship from its recovery in the 21st century: Role of the Indian Ocean SST anomaly associated with types of ENSO evolution." Geophysical Research Letters 48, no. 12 (2021): e2021GL092873.
88. Zheng, Yangxing, M. M. Ali, and Mark A. Bourassa. "Contribution of monthly and regional rainfall to the strength of Indian summer monsoon." Monthly Weather Review 144, no. 9 (2016): 3037-3055.
89. Zheng, Yangxing, Mark A. Bourassa, and M. M. Ali. "Statistical evidence on distinct impacts of short- and long-time fluctuations of Indian Ocean surface wind fields on Indian summer monsoon rainfall during 1991–2014." Climate Dynamics 54, no. 5 (2020): 3053-3076.

8. Declarations

Acknowledgements:

We acknowledge India Meteorological Department, National Oceanic and Atmospheric Administration, Copernicus Marine Environment Monitoring Service, Royal Netherlands Meteorological Institute, and National Centers for Environmental Prediction for providing data used in the study. The author(s) wish to acknowledge the use of the Ferret program for analysis and graphics in this paper. Ferret is a product of NOAA's Pacific Marine Environmental Laboratory. (Information is available at http://ferret.pmel.noaa.gov/Ferret/). We acknowledge the Department of Earth Sciences, Uppsala University, Uppsala and Indian National Centre for Ocean Information Services-ESSO, Ministry of Earth Sciences, Govt. of India, Hyderabad, India.

Author information

Affiliations

Department of Earth Sciences, Uppsala University, Uppsala, Sweden.

Venugopal Thandlam, Erik Sahlee, Anna Rutgersson

Department of Meteorology and Oceanography, Andhra University, Visakhapatnam, India.

S.S.V.S Ramakrishna, Venugopal Thandlam

The Center for Environment and Development Studies Research Forum, Uppsala University, Uppsala, Sweden.

Venugopal Thandlam

Indian National Centre for Ocean Information Services, Ministry of Earth Sciences, Hyderabad, India.

Hasibur Rahaman

Centre of Natural Hazards and Disaster Science, Uppsala University, Uppsala, Sweden.

Anna Rutgersson

National Centre for Polar and Ocean Research, Goa, India.

M.Ravichandran

Funding statement

We acknowledge the Department of Earth Sciences, Uppsala University, and the Swedish Research Council (VR) nr 2017-03988 for supporting this study.

Contributions

V.T: Conceptualization, methodology, formal analysis, visualization, writing-original draft, writing-review and editing; H.R: R.L.S.: Conceptualization, methodology, writing-review and editing; A.R: funding acquisition, review and editing, E.S: writing-review and editing; M.R: review and editing; R.K: review and editing.

Corresponding author

Correspondence to Venugopal Thandlam.

Ethics declarations

The manuscript has not been submitted to more than one journal for simultaneous consideration. The manuscript has not been published previously (partly or in full) unless the new work concerns an expansion of previous work. Our study is not split up into several parts to increase the number of submissions and submitted to various journals or to one journal over time. No data has been fabricated or manipulated (including images) to support our conclusions. No data or text by others are presented as if they were our own (“plagiarism”).

Competing interests

The authors declare no competing interests.

Figures

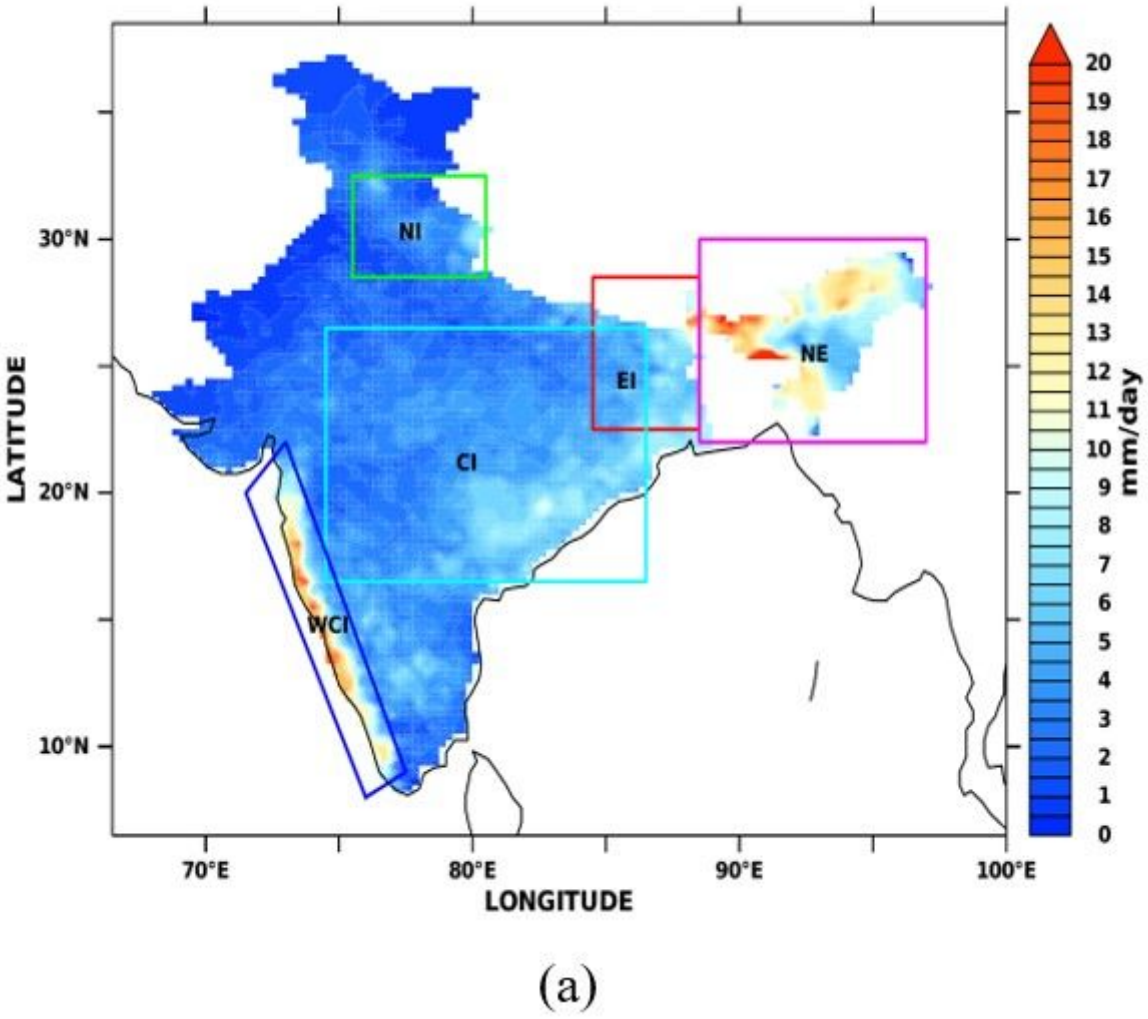

Figure 1

The climatology of AISMR (June-September) during 1993-2019 in colour and the homogeneous rainfall regions represented in rectangular boxes.

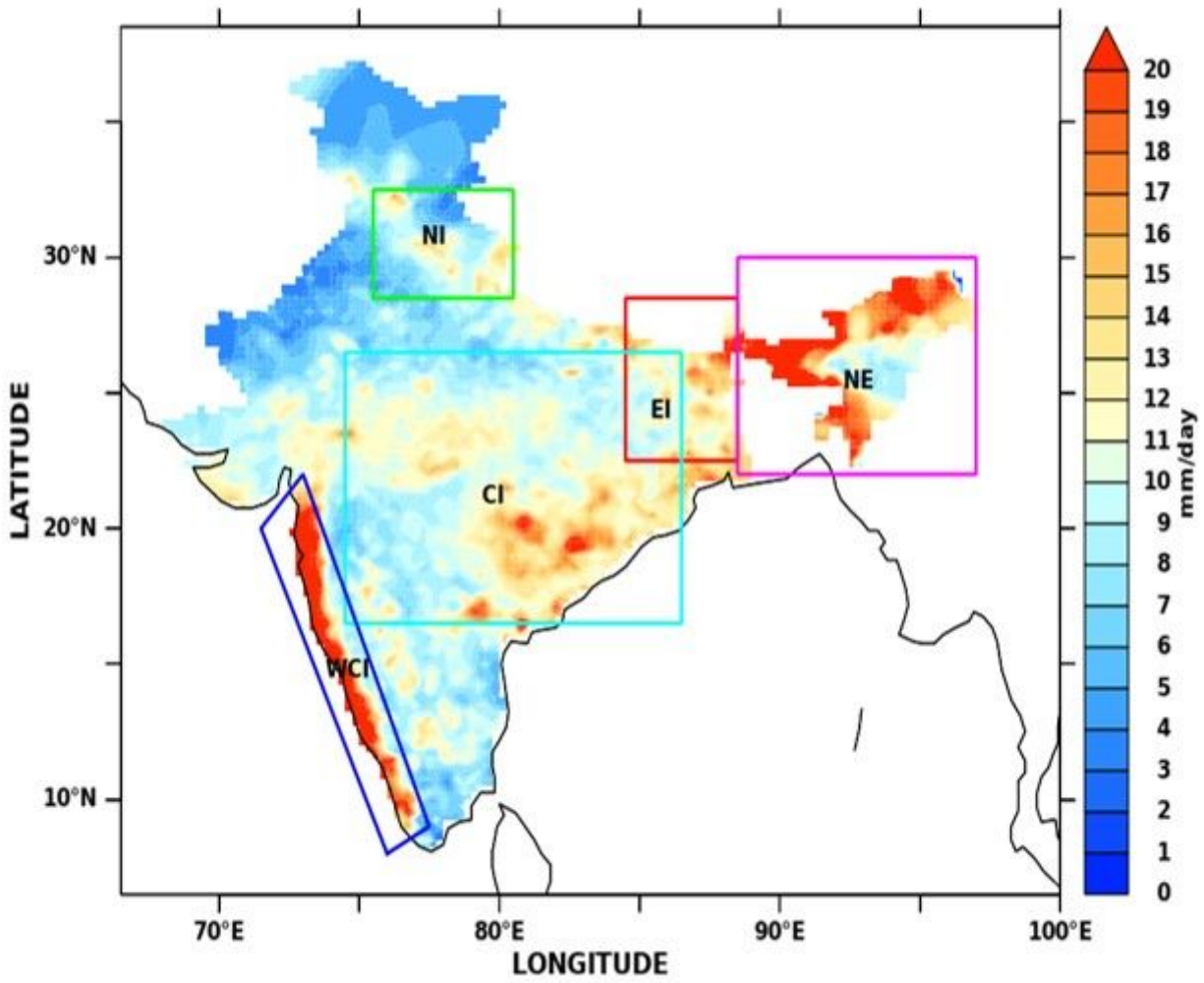

Figure 2

Spatial pattern of summer monsoon rainfall standard deviation (mm/day) during 1993-2019.

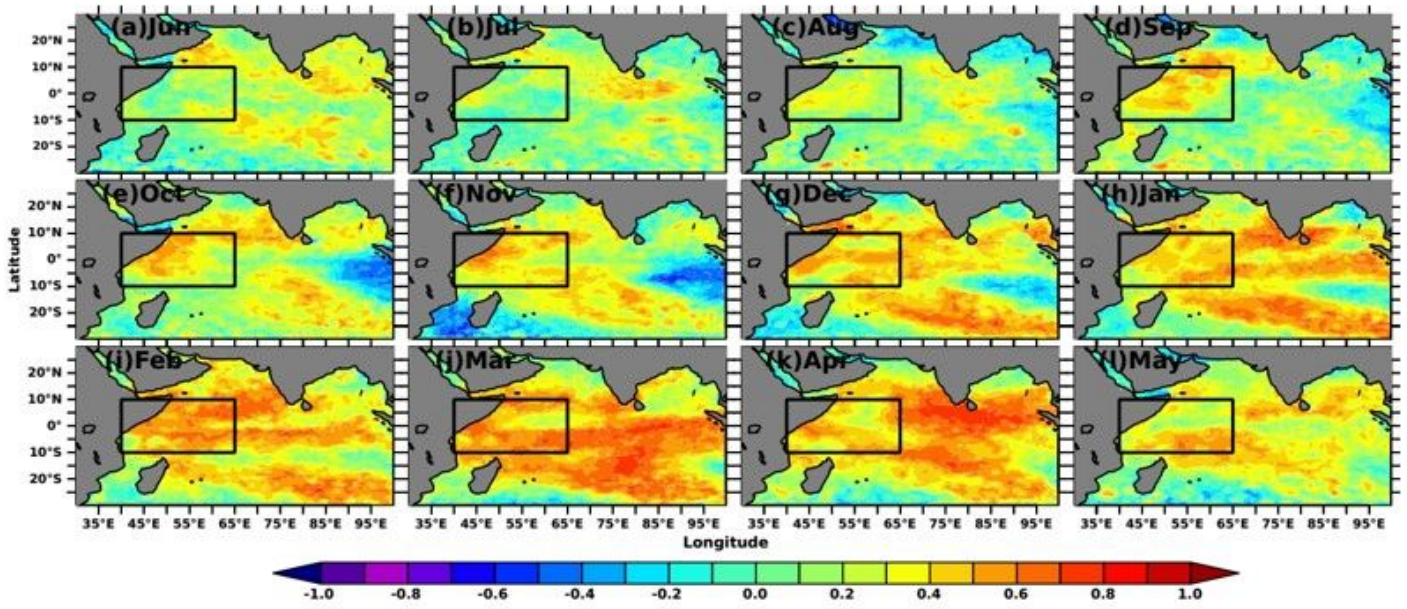

(a)

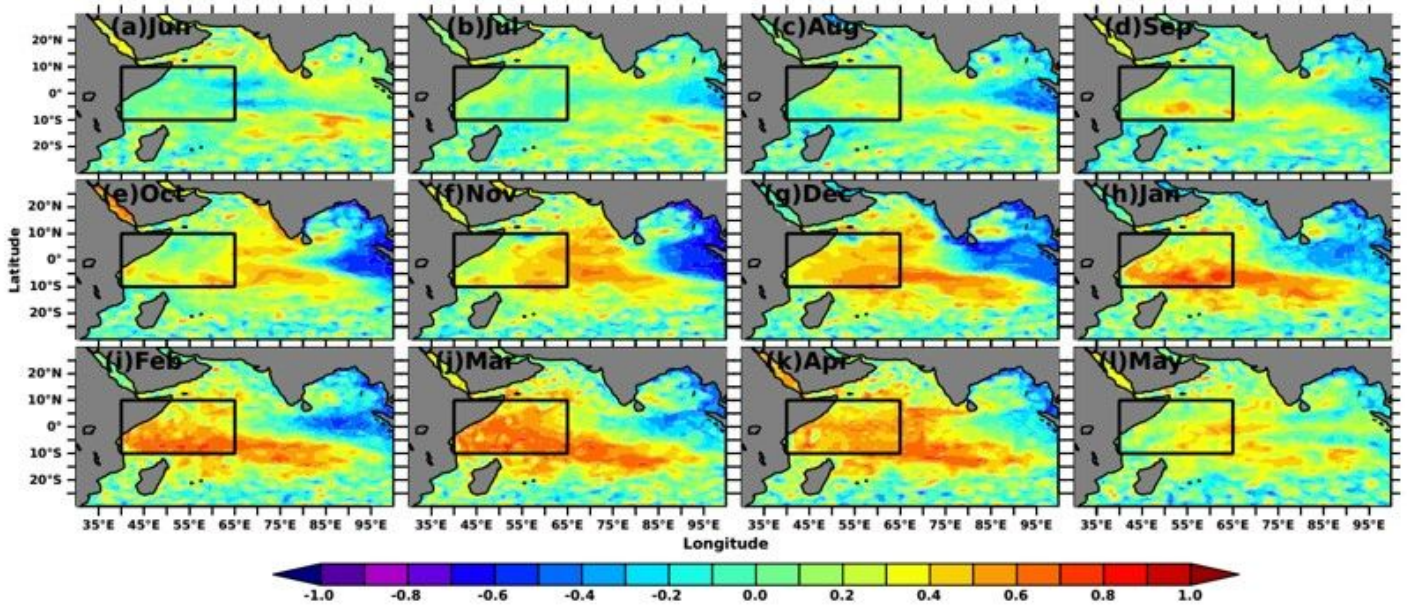

(b)

Figure 3

Simultaneous monthly correlations between (a) Indian Ocean SSTA and (b) Indian Ocean MSLA with Nino3.4 SSTA indices. The black rectangular box shows the correlations over SWIO. Correlations above +/- 0.2 are significant at 95%.

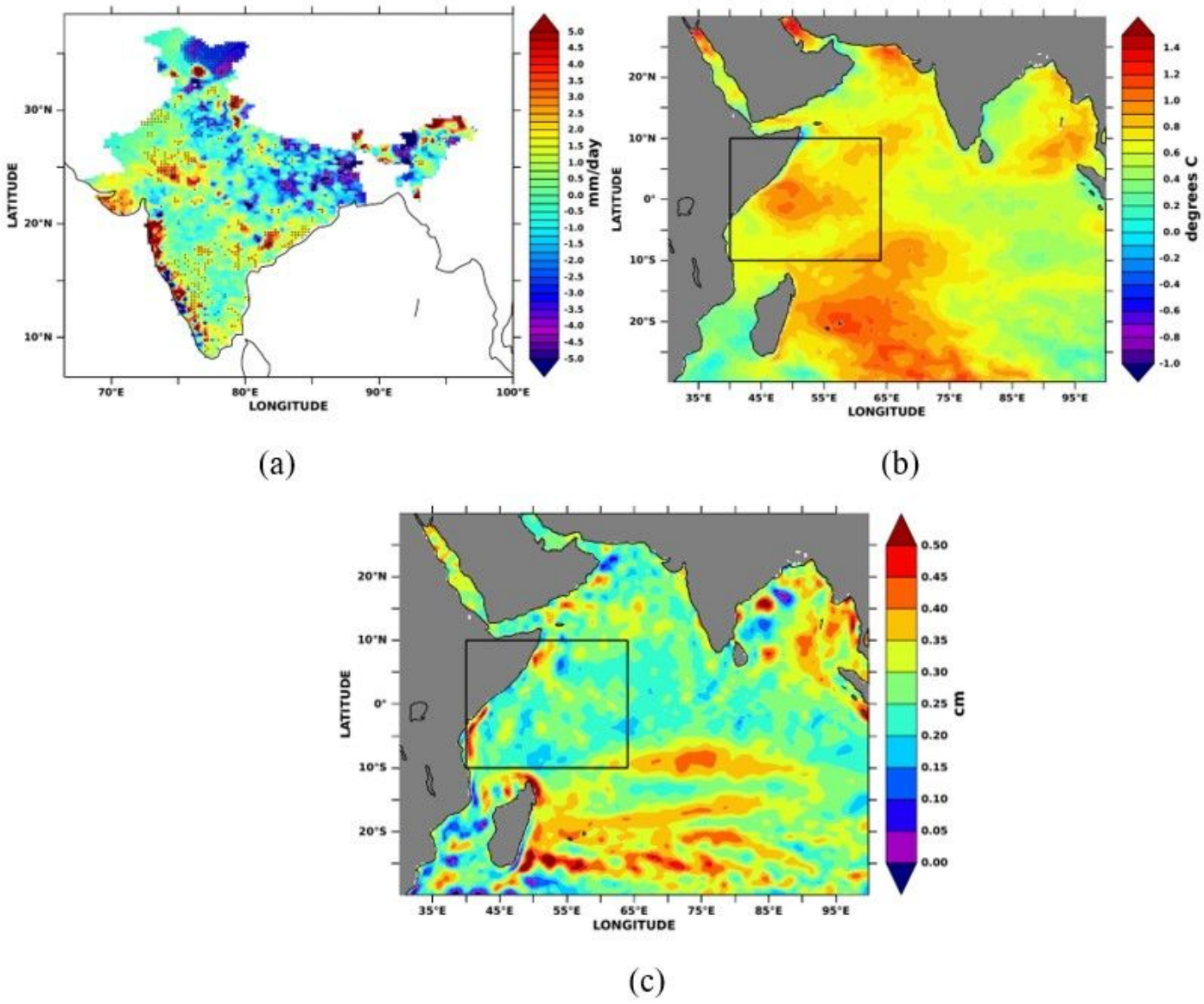

Figure 4

Total change (linear trend) in (a) AISMR, 90% significance trend is marked with black dots, (b) SST, and (c) SLA during 1993-2019. Both SST and SLA trends are significant at 99% over the majority of grids, hence not highlighted in the figure.

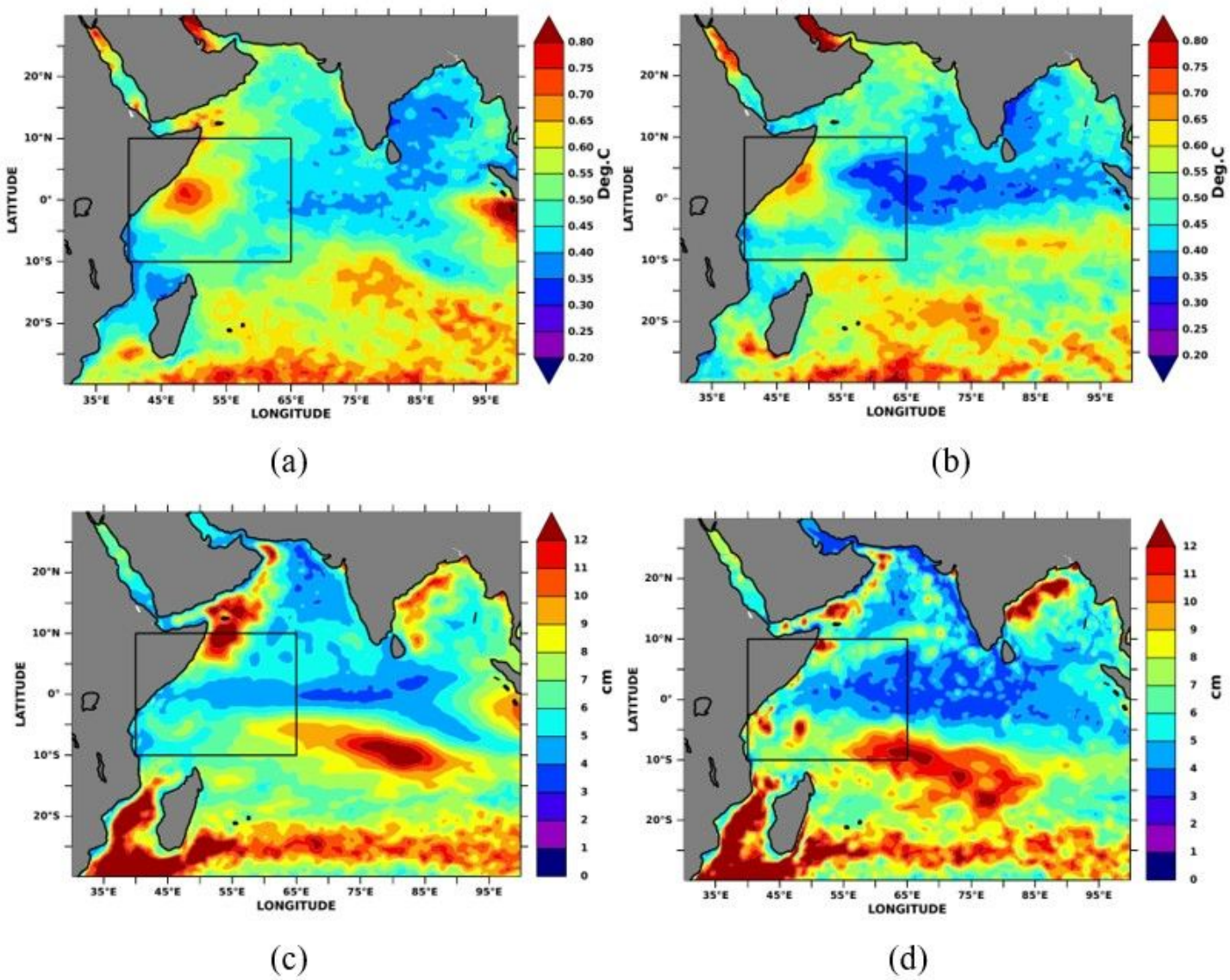

Figure 5

SSTA and MSLA standard deviation in the Indian Ocean. SSTA standard deviation during (a) winter half-year and (b) March-May. MSLA standard deviation during (c) winter-half year and (d) March-May.

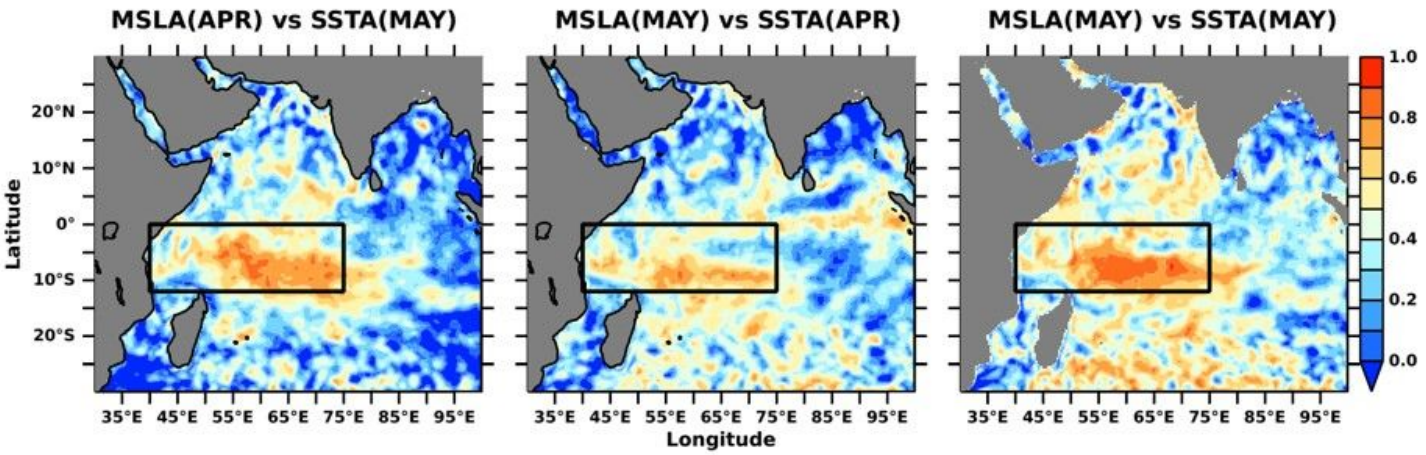

Figure 6

Spatial correlation of SSTA and MSLA during April-May

Figure 7

Lagged correlation of AISMR standard deviation with SSTA over the Indian Ocean. Values higher than +/- 0.2 significant at 95%.

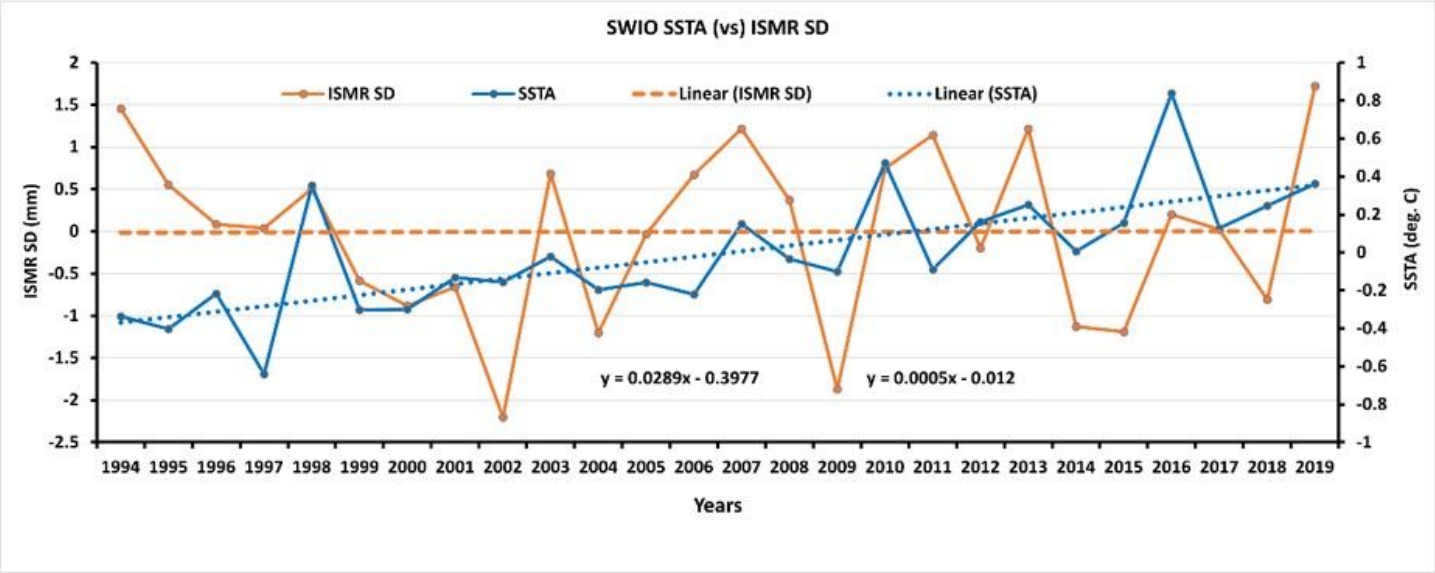

Figure 8

The time series of SSTA (solid blue line) over SWIO and AISMR standard deviation (solid orange line). Blue and orange dotted lines represent the SSTA and AISMR standard deviation trends, respectively.

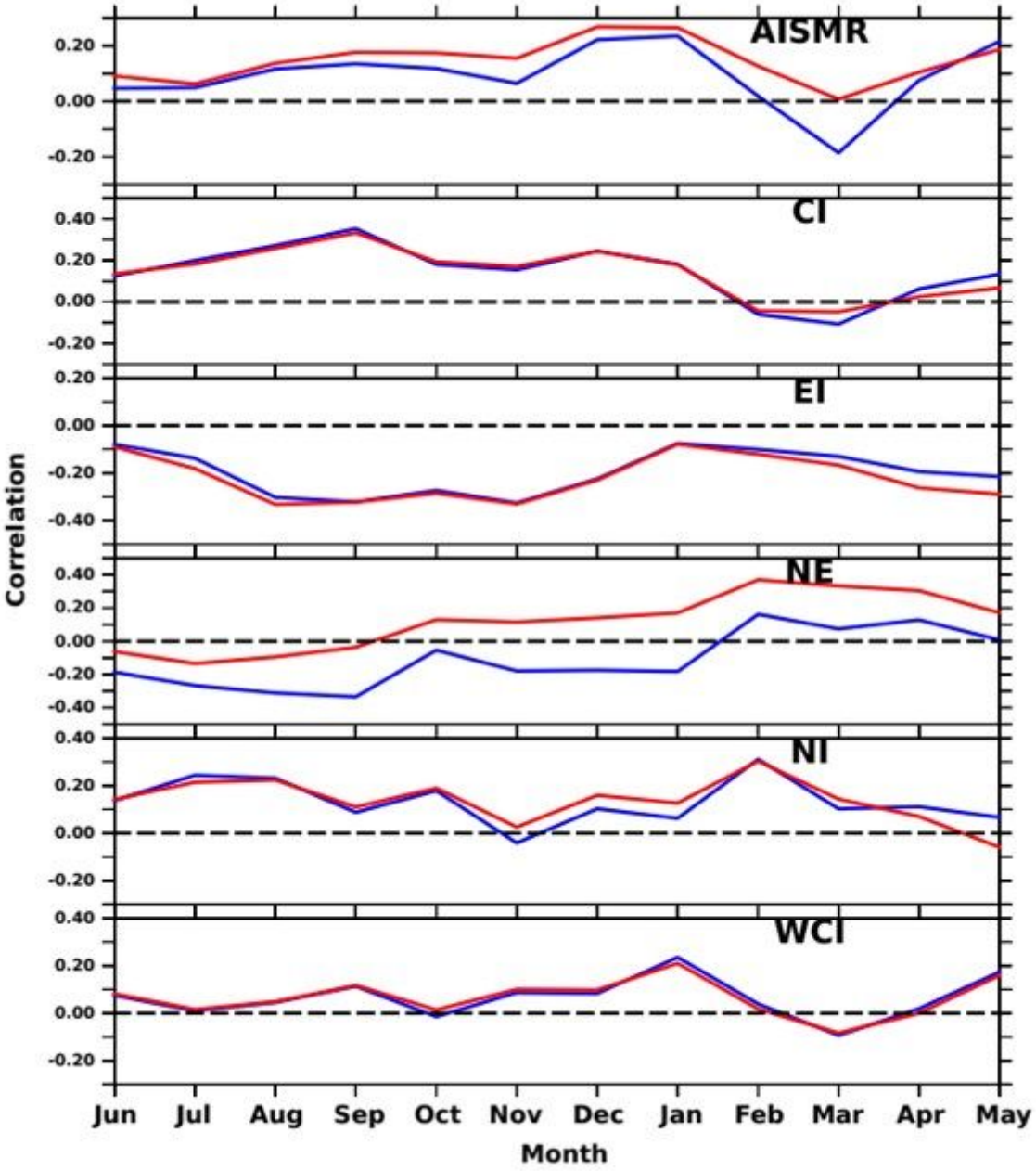

Figure 9

Time series of lagged correlation between SSTA over SWIO and regional rainfall over the five homogeneous regions and entire Indian landmass before (red) and after (blue) removing ENSO effect.

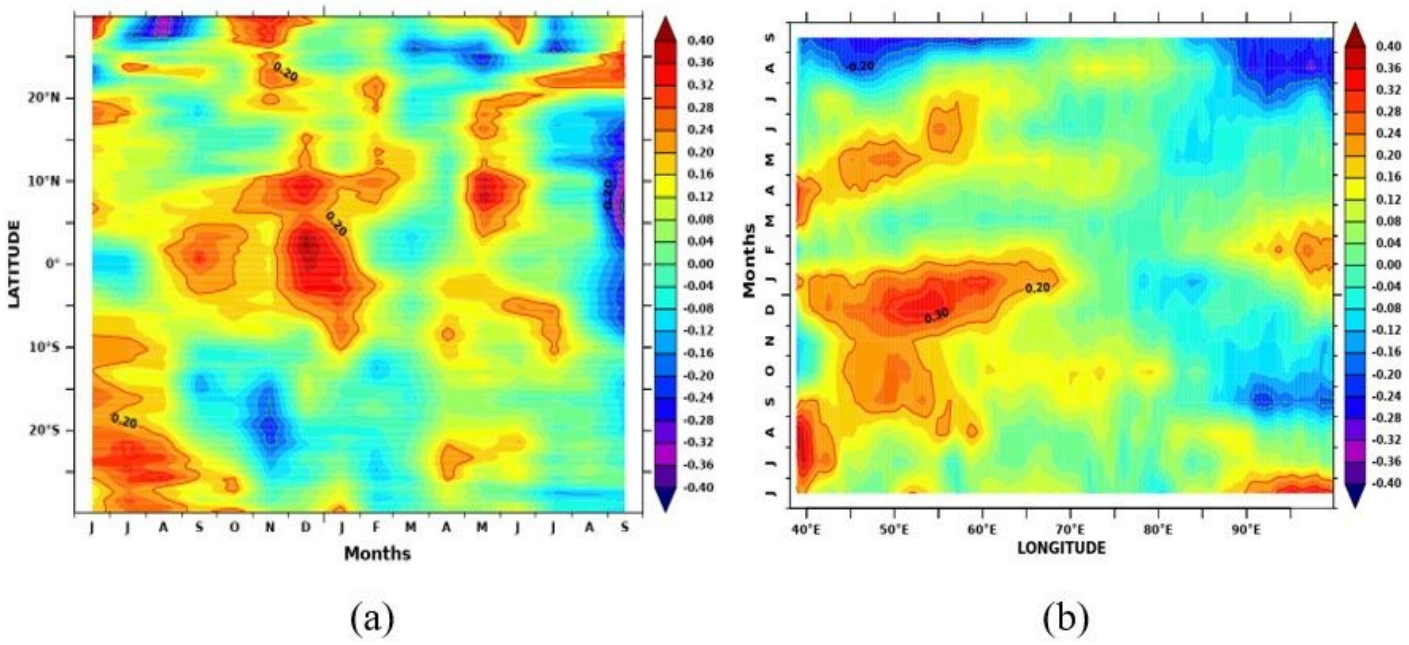

Figure 10

(a) Monthly lagged cross-correlation between AISMR standard deviation and SSTA averaged over 40-65E and (b) over 10S-10N.

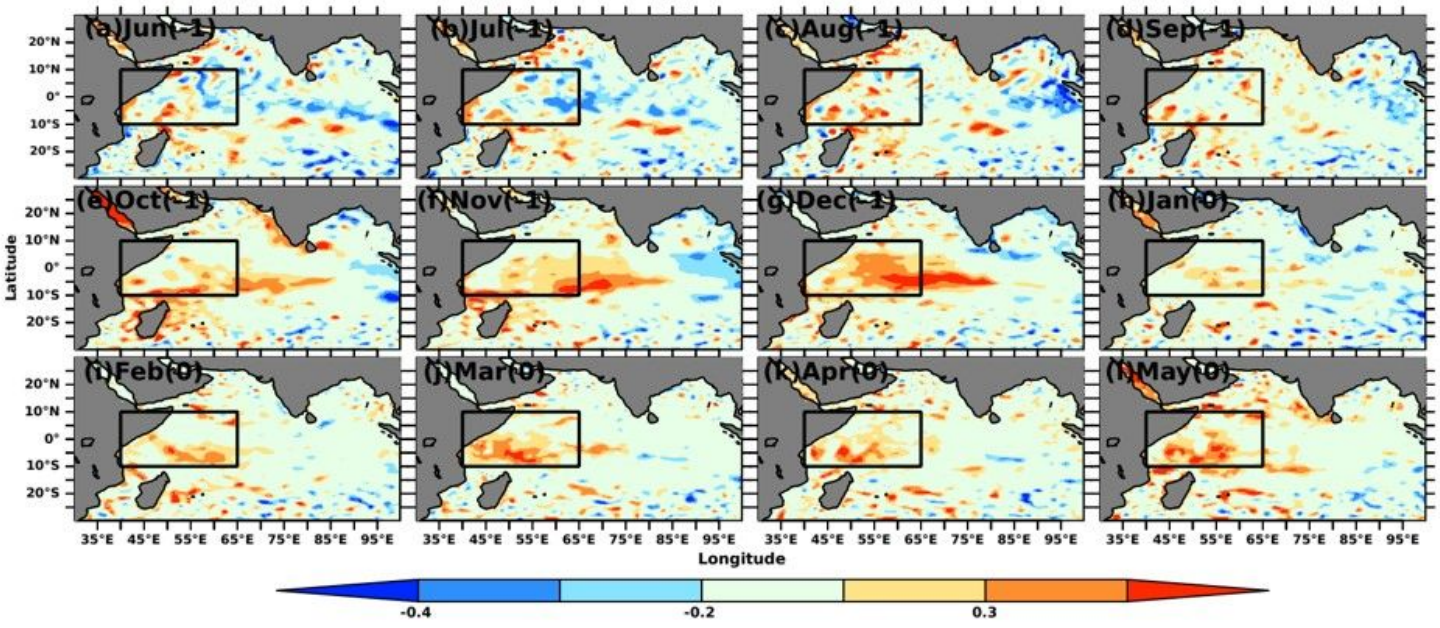

Figure 11

Lagged correlation of AISMR standard deviation with SSTA over the Indian Ocean. Values higher than +/- 0.2 significant at 90%.

Figure 12

The time series of MSLA (solid green line) over SWIO and AISMR standard deviation (solid orange line). The green dotted line represents the trend in MSLA.

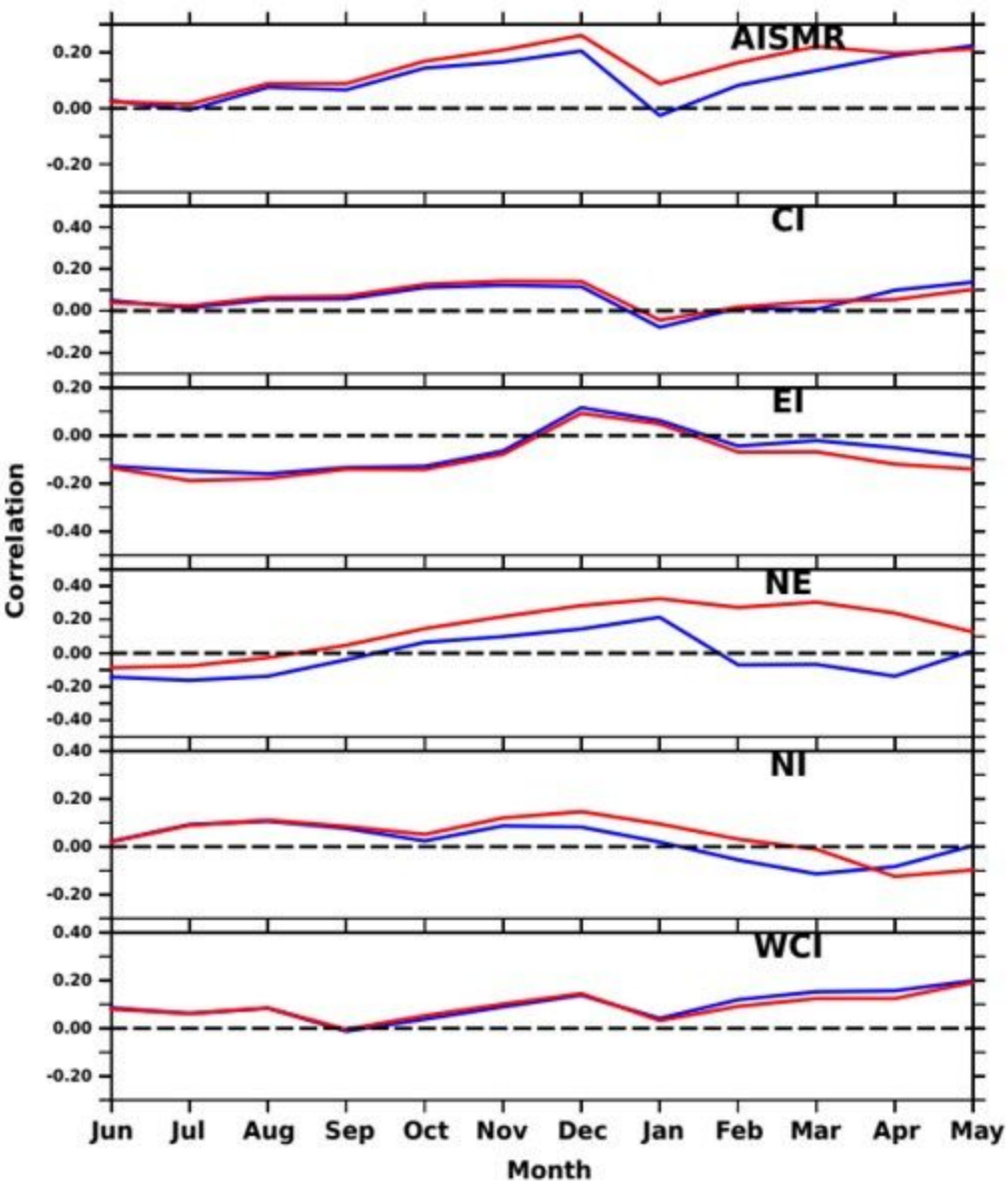

Figure 13

Time series of lagged correlation between MSLA over SWIO and regional rainfall over the five homogeneous regions and entire Indian landmass before (red) and after (blue) removing ENSO effect.

Figure 14

(a) Monthly lagged cross-correlation between AISMR standard deviation and SSTA averaged over 40-65E and (b) over 10S-10N.

Figure 15

Composite of May month's (a) SSTA and (b) MSLA variability (shaded) overlayed with wind anomalies (vectors) over the Indian Ocean during excess, deficit, and normal monsoon years.

Supplementary Files

This is a list of supplementary files associated with this preprint. Click to download.

- supplementarymaterial.docx